Politecnico di Torino

Politecnico di Torino

Master's Degree in Energy and Nuclear Engineering

Academic Year 2025/2026

Graduation Session March/April 2026

A Monte Carlo Study of Reactivity Equivalence in Fresh Fuel Storage and Spent Fuel Pool Criticality Analysis

Applicability and Limitations for Use in Storage Capacity and Criticality Safety Calculations

Supervisors:

Prof. Sandra Dulla

Prof. Jan Dufek

Dr. Sergiy Chernitskiy

Candidate:

Sara Di Siena

Author

Sara Di Siena, <s323115@studenti.polito.it sarads@kth.se>
Double Degree Nuclear Energy Engineering
Politecnico di Torino & KTH Royal Institute of Technology

Place for Project

Westinghouse Electric Sweden AB, Västerås, Sweden
KTH Royal Institute of Technology, Stockholm, Sweden

Politecnico di Torino Supervisor

Professor Sandra Dulla
Torino
Politecnico di Torino

KTH Supervisor

Associate Professor Jan Dufek
Stockholm
KTH Royal Institute of Technology

Westinghouse Supervisor

Sergiy Chernitskiy
Västerås
Westinghouse Electric Sweden AB

Abstract

The nuclear industry's transition toward higher fuel enrichments, aimed at improving fuel cycle economics and reducing waste volumes, requires rigorous criticality safety assessments to justify the use of existing storage infrastructure. A widely used licensing approach, the Reactivity Equivalence Method, assumes that fuel assemblies with higher enrichment and burnable absorbers are safe for storage if their infinite multiplication factor k_∞ in a simplified core geometry matches that of a licensed reference fuel. This thesis evaluates the validity of this method for a VVER-1000 fuel assembly containing gadolinium rods within Fresh Fuel Storage Container and Spent Fuel Pool (SFP) configurations, utilizing continuous-energy Monte Carlo (MCNP 6.2) simulations. The study demonstrates that the Reactivity Equivalence Method is both non-conservative and unreliable when applied to these storage environments. Numerical results indicate that *equivalent* gadolinium-bearing assemblies yield consistently higher effective multiplication factors k_{eff} in storage geometries than the reference fuel. Detailed spectral analysis identifies two fundamental physical mechanisms driving this failure: a nonlinear competition between $^{235}\mathrm{U}$ fission and Gd absorption in softer neutron spectra, and a spatial thermal flux inversion driven by external moderation. This flux inversion causes a reversal in the effectiveness ranking of absorber patterns, leading the simplified core model to misidentify the bounding worst-case configuration. Additionally, in the SFP, competitive absorption between internal gadolinium rods and external borated storage racks further diminishes absorber worth, compounding the safety margin erosion. Consequently, this work concludes that criticality safety analyses for systems involving spectrally sensitive absorbers must utilize high-fidelity 3D models that accurately capture the specific spectral and spatial conditions of the storage environment.

Keywords

Criticality Safety, Reactivity Equivalence, Burnable Absorbers, Gadolinium, MCNP, Spent Fuel Pool, Neutron Spectrum, VVER-1000.

This page intentionally left blank.

Acknowledgments

I would like to express my sincere gratitude to everyone who has supported me during the course of this Master's thesis.

First, I am very grateful to Westinghouse Electric Sweden for giving me the opportunity to carry out this work. I would especially like to thank my manager, Christofer Willman, for welcoming me into such an engaging and professional environment and for placing his trust in me. My deepest gratitude goes to my industrial supervisor, Sergiy Chernitskiy. This thesis would not have been possible without your expert guidance and the generous amount of time you dedicated to my learning. Thank you for your patience in answering my daily questions, for teaching me the intricacies of criticality safety, and for always challenging me to deepen my understanding of the physics behind the results. Your mentorship has been invaluable to my professional growth.

I would also like to thank my academic supervisor at KTH, Professor Jan Dufek, for his guidance, valuable feedback, and for ensuring the academic quality of this work.

I extend my gratitude to Professor Sandra Dulla at Politecnico di Torino for her academic supervision and for overseeing my path during this double degree program.

Finally, I am deeply thankful to my friends and family for their constant encouragement and support during my studies.

This page intentionally left blank.

Contents

List of Acronyms

BA Burnable Absorber. 11, 12, 14, 20, 22, 33, 37

BWR Boiling Water Reactor. 5

CI Confidence Interval. , 18, 23, 26, 27, 29, 30

FA Fuel Assembly. , 1, 5, 6, 8, 9, 11, 12, 14–16, 20, 21, 23, 36, 37

IFBA Integral Fuel Burnable Absorber. 12

LWR Light Water Reactor. 12, 15

MCNP Monte Carlo N-Particle Transport Code. 2–4, 15–19, 22

NRC US Nuclear Regulatory Commission. 6

PWR Pressurized Water Reactor. 5

RWFA Robust Westinghouse Fuel Assembly. 3, 15, 16, 33

SFP Spent Fuel Pool. , 1–4, 6, 9, 15, 16, 18, 20, 21, 29, 31–33, 35, 37, 39

USL Upper Subcritical Limit. 8

VVER Russian Pressurized Water Reactor. 3, 5, 16

List of Figures

List of Tables

This page intentionally left blank.

1 Introduction

1.1 Context and Motivation

The commercial nuclear power industry is continuously evolving to improve fuel cycle economics, operational flexibility, and resource utilization. A primary driver for this evolution is the industry-wide trend toward higher fuel enrichments. This increase in initial enrichment allows for longer operating cycles, higher fuel burnup, and a reduction in the total volume of spent fuel produced per unit of energy generated.

While this trend offers clear advantages for in-core reactor performance, it introduces a significant challenge for the rest of the nuclear fuel cycle. Specifically, this higher-enrichment fuel must be safely manufactured, transported, and stored in existing facilities. These auxiliary systems, such as fresh fuel storage containers and Spent Fuel Pools (SFPs), were often designed and licensed for fuel with lower enrichments.

To justify the storage of new, higher-enrichment Fuel Assemblies (FAs) in these existing facilities, operators often rely on the establishment of reactivity equivalence relations. This thesis focuses on a procedure that establishes equivalence within a reference core geometry to take credit for the presence of integrated burnable absorbers, which will be hereafter referred to as the *Reactivity Equivalence Method*. This comparative approach, which has been investigated and utilized within the nuclear industry [1] [2], is intended to demonstrate that a new fuel configuration is as safe as, or safer than, the original licensed design.

1.2 Problem Description

The Reactivity Equivalence Method is typically based on a simplified model. It aims to show that a new FA, for instance one with higher $^{235}\mathrm{U}$ enrichment and fixed neutron absorbers like gadolinium-bearing rods, is *reactively equivalent* to the original lower-enrichment reference fuel. This equivalence is commonly established by showing that the new fuel's infinite multiplication factor (k_∞) in a 2D reference geometry, often representing the in-core environment, is less than or equal to that of the reference fuel.

The central hypothesis of this thesis is that this widely-used Reactivity Equivalence Method may be fundamentally flawed and non-conservative for out-of-core storage applications. The method relies on a critical, and often unstated, assumption: that the neutronic behavior of the two fuel types will scale predictably when moved from the idealized core model to the actual storage geometry. This assumption is questionable because the neutronic environments are drastically different.

The key physical mechanism behind this potential failure is the discrepancy in moderation, which alters the neutron spectrum. The reactivity worth of a neutron absorber like gadolinium is extremely sensitive to the neutron energy spectrum, as its absorption cross-section is orders of magnitude higher at thermal energies. This spectral sensitivity forms the basis of the thesis hypothesis: that a simplified model may fail to accurately predict the complex, non-linear reactivity effects that arise in storage configurations. The potential for error is further amplified in a SFP, where it is uncertain whether a two-dimensional model can adequately capture the competitive absorption between gadolinium in the fuel and boron in the external storage racks.

1.3 Literature Review

The analysis of criticality safety in SFPs and storage containers has evolved significantly in response to the industry's transition toward higher fuel enrichment and burnup limits. Consequently, recent research has increasingly examined the limitations of simplified modeling assumptions when applied to realistic storage geometries.

Current industry guidance, such as NEI 12-16 [3], establishes the standards required for performing criticality analyses of fuel storage systems. This guidance emphasizes the need for explicit geometric modeling and the validation of computational methods for specific neutronic configurations, including the consideration of manufacturing tolerances and optimum moderation conditions to ensure bounding safety margins.

Monte Carlo codes, particularly Monte Carlo N-Particle Transport Code (MCNP) [4], have become the industry standard for meeting these requirements due to their ability to model heterogeneous geometries without homogenization errors. For example, Cho et al. (2025) [5] employed MCNP to investigate the reactivity effects of eccentric loading in spent fuel casks, demonstrating that geometric deviations can result in non-negligible reactivity increases.

Another critical area of investigation concerns the complex interplay between moderator density and neutron spectral shifts. In a highly relevant study, Park et al. (2025) [6] analyzed optimum moderation conditions in new fuel storage vaults. Their work provides quantitative evidence that reduced moderator density induces significant spectral hardening and elongates the neutron mean free path. Crucially, they demonstrated that these physical changes lead to reactivity peaks that simplified models fail to capture, thereby challenging the validity of assuming linear or predictable behavior across different moderation regimes.

Despite the emphasis on explicit modeling in standards such as NEI 12-16, reactivity equivalence relations continue to be explored as a means to simplify licensing by relating non-reference fuel configurations to standard reference designs. These methods typically rely on a standard cold core geometry, as defined in NUREG/CR-7194 [1]. However, Neuber (1999) [2] identified limitations in applying equivalence relations across different geometries, noting that spectral differences can invalidate such transfers.

This thesis addresses the gap between simplified reactivity equivalence methods and the modeling rigor required for modern VVER-1000 fuel designs containing integral burnable absorbers.

1.4 Objectives and Research Questions

This thesis aims to assess, via Monte Carlo simulations, the applicability, limitations, and potential non-conservatism of the Reactivity Equivalence Method for fresh and spent fuel criticality safety analyses.

To achieve this objective, this work will answer the following specific research questions:

- Is the Reactivity Equivalence Method, based on an in-core k_∞ comparison, a conservative approach for the criticality safety analysis of a fresh fuel storage container?
- How do changes in the neutron energy spectrum between core and storage geometries affect the reactivity of gadolinium-bearing fuel rods?
- Does the *most reactive* absorber configuration identified in a simplified core model match the most reactive configuration in the full 3D storage model?
- Does the method remain valid for a complex SFP environment that includes competitive absorption between gadolinium in the fuel and boron in the storage racks?

1.5 Scope and Limitations

This study is subject to the following scope and limitations:

- The analysis focuses on a specific Russian Pressurized Water Reactor (VVER)-1000 Robust Westinghouse Fuel Assembly (RWFA)-T design.
- The study analyzes fresh (unirradiated) fuel only. No credit is taken for the reactivity changes resulting from fuel burnup.
- All criticality calculations are performed using the MCNP code, version 6.2.
- To protect proprietary information, specific data related to the commercial designs from Westinghouse Electric Sweden AB are omitted from this public report.

1.6 Structure of the Thesis

This thesis is organized into six chapters.

Chapter 2, “Background”, provides the theoretical foundation for the study. It covers the fundamentals of the nuclear fuel cycle, the principles of criticality safety, and the physics of burnable absorbers, with a specific focus on gadolinium.

Chapter 3, “Methodology”, describes the computational models and the analytical procedure. It details the MCNP models for the fuel assembly, the fresh fuel container, the SFP, and the idealized core geometry. It also outlines the step-by-step evaluation procedure used to test the Reactivity Equivalence Method.

Chapter 4, “Results”, presents the numerical results from the MCNP simulations. It establishes the reference case and provides a direct comparison of the reactivity of the *equivalent* fuel in the different geometries, identifying the key failures of the method.

Chapter 5, “Discussion”, provides a physical interpretation of the data presented in the results. It explains *why* the method fails by analyzing the neutron spectrum and the absorber rank inconsistency, and it discusses the implications of these findings for criticality safety.

Chapter 6, “Conclusion”. summarizes the main findings of the thesis, directly answers the research questions, and provides final recommendations.

2 Background

2.1 The Nuclear Fuel Cycle

Nuclear power currently accounts for around 10% of global electricity generation, providing a low-carbon and reliable energy source [7]. The nuclear fuel cycle includes all the stages associated with the production of nuclear energy. It spans from uranium extraction to the final disposal of spent fuel. It can be divided into two main parts, with reactor irradiation as the dividing point: the *front end*, which covers all the steps from uranium mining to fresh fuel storage, and the *back end*, which deals with spent fuel and waste management.

Uranium is typically found as an oxide/metal embedded in rock. Therefore, the first step of the cycle consists in its mining, which can be carried out using open-pit mining, underground mining, or in-situ leaching, depending on the characteristics of the ore-bearing zone. Afterwards, the uranium ore is concentrated into the so-called *yellowcake*, a powder of uranium in the form of U_3O_8.

As most energy producing reactors operate on enriched uranium, the yellowcake has to be converted into a form which is suitable for transport and to be used as an input for the enrichment process, which generally requires the uranium feed to be in a gaseous form. U_3O_8 is usually converted into UF_6, which is solid at room temperature and gaseous above $56.5\,^{\circ}\mathrm{C}$ at atmospheric pressure [8]. The enrichment process can be carried out using several technologies, including gas centrifuge, gas diffusion, or laser excitation. However, gas centrifuges are typically preferred because they are more economical than laser excitation and require fewer stages than gas diffusion to achieve the enrichment level required by the reactor design.

Once enriched, UF_6 is transported to fuel fabrication plants, where it is converted into uranium dioxide (UO_2) powder and processed into fuel pellets and assemblies. One of these facilities is located in Västerås, Sweden. It is one of Westinghouse's three fuel fabrication plants and the only such facility in the Nordic region. The Västerås plant is also the only one worldwide that manufactures all three major fuel types, i.e. for Pressurized Water Reactors (PWRs), Boiling Water Reactors (BWRs), and VVERs. In Västerås, UF_6 is converted into UO_2, pressed into pellets, sintered at high temperature, and loaded into zirconium alloy tubes to form fuel rods [9]. Some rods incorporate gadolinium-bearing pellets to help control the power distribution in the reactor and optimize fuel utilization. The rods are then assembled into the FAs, which are subsequently transported to nuclear power plants for storage prior to core loading.

After the residency in the reactor for a predetermined amount of power cycles, the FAs that are unloaded from the core contain fission products, minor actinides,

and residual fissile material. Therefore, they must be managed safely due to both their radiological hazard and potential for criticality. According to the US Nuclear Regulatory Commission (NRC), the only two acceptable storage methods for irradiated fuel are SFPs, followed by dry cask storage [10]. In countries other than the US, reprocessing might also be permitted by national regulations.

The SFPs used for this initial storage are usually located in the reactor containment building. They are filled with water equipped with active cooling systems to provide both cooling and shielding for the spent FAs during the phase in which both the activity and the decay heat production are significant.

After this wet storage stage, the fuel is typically transferred to an interim dry storage facility, which is often designed for a licensed operational lifetime of up to 100 years. The long-term management strategy for the spent fuel, such as permanent disposal in a geological repository, has not yet been finalized in many countries [11].

2.2 Fundamentals of Criticality and Criticality Safety

The central focus of this thesis is the criticality analysis of fresh and spent fuel storage systems. This section presents the theoretical framework that supports the analyses and methodologies discussed in the following chapters.

The fundamental reaction behind criticality is nuclear fission. Fission can occur spontaneously in certain unstable nuclides or, more commonly, can be induced by the absorption of a neutron. In the latter case, the incident neutron causes the nucleus to split into two lighter fragments (i.e. the fission products), releasing energy and emitting additional neutrons that can sustain a chain reaction.

The probability that an incident neutron will induce fission in a nucleus is described by its fission cross-section σ_f, which depends on the energy of the incident neutron. Figure 1 shows the energy dependency of the fission cross section σ_f of the most used fissile material, $^{235}\mathrm{U}$. The neutron energy spectrum has therefore a critical influence on the efficiency of the chain reaction.

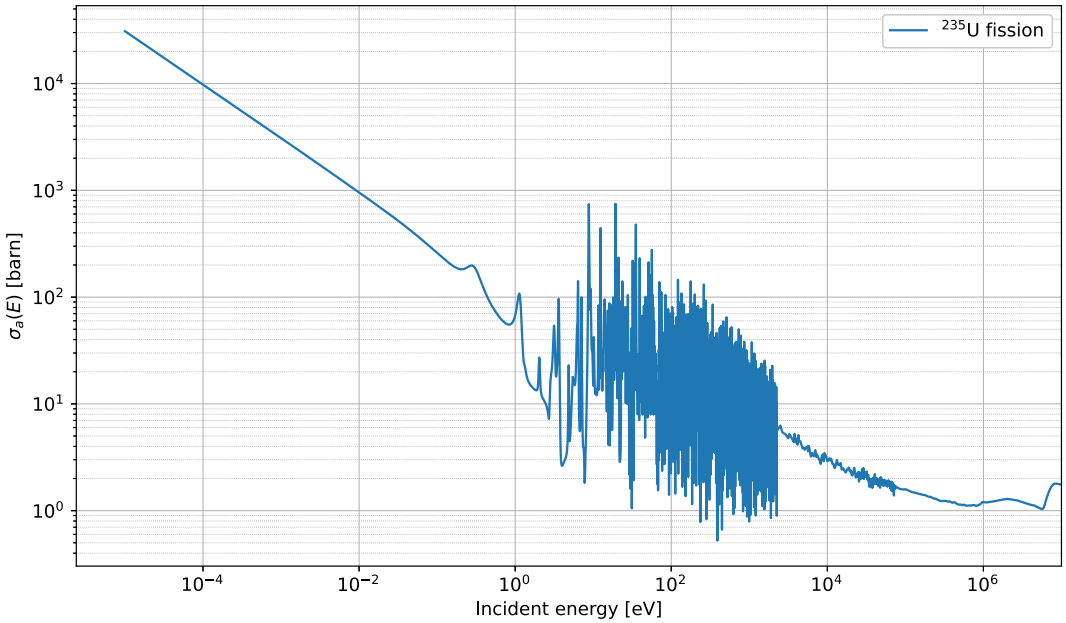

Figure 1: Fission cross section for ^{235}U, as a function of incident neutron energy. Data obtained from the ENDF/B-VIII.0 library [12].

The key parameter describing the behavior of the chain reaction is the effective multiplication factor k_{eff}, defined as follows:

$$k_{\text{eff}} = \frac{N_{m+1}}{N_m}, \tag{2.1}$$

where N_m and N_{m+1} are the number of neutrons in generation m and $m+1$, respectively [13].

If $k_{\text{eff}} = 1$, the number of fissions (and, as a consequence, the produced power) remains constant and the nuclear chain reaction is self-sustaining. If $k_{\text{eff}} < 1$, the system is subcritical and the number of fission reactions decreases over time. Conversely, when $k_{\text{eff}} > 1$, the system becomes supercritical. In this case, the number of fissions and the power production increase exponentially.

Criticality safety aims at avoiding unintended criticality in fissile material systems where a chain reaction could occur. This is obtained by means of maintaining k_{eff} below a defined subcritical limit with an appropriate margin, accounting for uncertainties and potential abnormal conditions. The k_{eff} of a system depends on

- the characteristics of the fissile material, such as its mass, concentration, nuclide composition, chemical form, temperature and density;
- its geometry;
- the presence in the system of moderating, absorbing or reflecting materials.

Criticality safety can be achieved by controlling these parameters by means of en-

gineered and/or administrative measures. Limits on these parameters that guarantee subcriticality in the system must be evaluated using a conservative approach.

The maximum calculated k_{eff} value that is considered to be safely subcritical can be referred to as Upper Subcritical Limit (USL). It accounts for all relevant uncertainty and bias. These include uncertainties in nuclear data, bias identified by validating the calculation method against relevant critical benchmark experiments, the statistical uncertainty of the Monte Carlo code and uncertainties on conservative assumptions.

The IAEA Safety Guide SSG-27 [14] provides recommendations for ensuring subcriticality when handling fissile material, during both normal operational states and credible abnormal conditions. In common industrial and engineering practice, a conservative target of $k_{\text{eff}} < 0.95$ is set for normal operation, $k_{\text{eff}} \leq 0.95$ for abnormal operations (i.e. when a single failure occurs), and $k_{\text{eff}} \leq 0.98$ for scenarios in which two or more unlikely and independent failures occur concurrently. However, these limits might vary depending on the regulatory requirements and the methodology used for the criticality safety analysis.

2.3 Criticality Safety in Handling and Storage of Fresh Fuel

Unirradiated fuel can contain a relatively high inventory of fissile isotopes. In this analysis, only ^{235}U is considered as it is the only one used in the Västerås production plant. As mentioned in Section 2.1, FAs must be safely transported from fuel fabrication plants to nuclear power plants and then stored on-site prior to core loading. For this purpose, containers are usually employed. They are designed to guarantee mechanical integrity, shielding, and subcriticality under normal and credible accident scenarios. Since fresh fuel only generates an amount of decay heat that does not usually require any active cooling, dry storage environments are typically preferred. Furthermore, to increase operational flexibility, utilities sometimes wish to store or transport fresh fuel at enrichments higher than the reference limit. This can be achieved by inserting burnable absorbers (e.g., gadolinium-bearing rods) to reduce system reactivity and maintain subcriticality. Therefore, when designing and operating fresh fuel storage and handling systems, several design and safety aspects should be considered.

The IAEA recommends that these assessments be based on several key principles to ensure safety [14]:

- geometry, as minimum spacing between FAs and containers is essential to provide favourable neutron leakage and minimise the interaction between units;
- when applicable, surveillance of fixed solid absorbers is fundamental to make sure they are still effective and were not affected by displacement, corrosion or ageing beyond assumptions;
- the potential ingress of moderating water must be accounted for, as the containers and their storage area must be designed to ensure subcriticality even in the case of water flooding;

- administrative controls and procedures (e.g. verification that the fissile nuclide composition is within the criticality limitations of the area where it is intended to be stored) are essential to prevent accidental formation of critical configurations.

Criticality analyses for these configurations are typically performed assuming worst-case moderation (the so called *optimum moderation conditions*) and reflection, to ensure compliance with regulatory limits.

2.4 Criticality Safety in Spent Fuel Operations

Once discharged from the reactor core, FAs are transferred to the SFP, where they are stored temporarily to allow for initial cooling and radioactive decay. The minimum water depth is defined by the national regulatory requirements, and must be sufficient to provide adequate shielding to the working areas surrounding the pool. Active cooling of the FAs is provided inside the pool to extract decay heat, which is significant for several years after the removal of the fuel from the reactor. The assemblies are stored vertically in stainless steel racks that often contain boron to enhance neutron absorption and allow for a more compact rack configuration. In some designs, soluble boron in the pool water provides an additional subcriticality margin. However, many safety analyses are conservatively performed without taking credit for soluble boron.

The storage racks in SFPs are engineered to maintain subcriticality under both normal operating conditions and credible abnormal or accident scenarios, including events such as misloading, structural deformation, or changes in moderation. Maintaining subcriticality in the system presents unique challenges, as the isotopic composition and physical state of the fuel evolve during irradiation and subsequent decay, directly influencing its reactivity. Because these changes depend on irradiation history, accurately identifying the most reactive state of the fuel outside the reactor core is nontrivial. In addition, the most reactive geometry during storage does not necessarily coincide with that in the core. Variations in moderation and isotopic composition can result in a higher k_{eff} than at end-of-cycle. For this reason, criticality assessments must explicitly account for post-irradiation conditions that may increase reactivity.

To address these challenges, subcriticality is primarily ensured through geometrically favourable configurations, such as spacing and rack design, while fixed neutron absorbers and burnup credit are used as supplementary safety measures. Storage arrays must maintain subcriticality even in the presence of credible abnormal conditions, including handling errors, flooding, or FA misalignment, and regular inspections are required to prevent the inadvertent loss of favourable geometry. Where soluble absorbers like boron are employed, potential dilution events must be considered, and the long-term performance of fixed absorbers must be assessed for ageing or irradiation degradation. If burnup credit is applied, it must rely on validated depletion and criticality calculation methodologies, conservative isotopic assumptions, and allowances for axial and assembly-to-assembly burnup variations. Operations involving degraded fuel or transfers between wet and dry

storage environments demand additional administrative and engineered controls to avoid inadvertent increases in moderation or changes in configuration. These principles form the basis of criticality safety evaluations for spent fuel operations and provide the technical foundation for the analyses conducted in this thesis.

2.5 Criticality Incidents

A foundational principle of criticality safety is the analysis of past operational experience. Although modern storage systems for fresh and spent nuclear fuel possess an outstanding safety record, a review of historical criticality accidents offers crucial lessons on potential failure mechanisms, the role of human factors, and the importance of strict adherence to safety protocols. A comprehensive survey of such events is provided in the Los Alamos National Laboratory report, "A Review of Criticality Accidents" [15].

The vast majority of the 22 process-related accidents documented in the review occurred in facilities that handled fissile materials as liquids (i.e., solutions or slurries), where both the geometry and concentration were highly variable. These scenarios differ fundamentally from the storage of solid fuel assemblies within fixed-geometry containers or racks. However, these historical events enlighten fundamental principles of criticality control that remain highly relevant. To date, no major criticality accidents have been recorded in contemporary commercial spent fuel pools or dry cask storage systems. This fact alone underscores the effectiveness of passive safety designs that rely on fixed geometry and solid neutron absorbers. Nevertheless, a few specific incidents serve as important case studies for understanding potential risks.

The most significant criticality accident in recent history took place on September 30, 1999, at a fuel conversion facility in Tokai-mura, Japan [16]. The incident was initiated when workers, following an unauthorized and unwritten procedure to accelerate their work, handled a highly enriched uranyl nitrate solution improperly. They bypassed a geometrically favorable dissolution tower and instead poured the solution directly into a large-volume precipitation tank with an unsafe geometry. The amount of uranium in the tank exceeded by far the administrative mass limit. This action resulted in a self-sustaining fission chain reaction that persisted for about 20 hours. It led to two fatalities due to acute radiation syndrome and caused significant radiation exposure to another employee, as well as to members of the public in the vicinity. The excursion was only terminated after the cooling water jacket that surrounded the precipitation tank was drained, thereby removing a key neutron reflector. The Tokai-mura event is a stark reminder that even in a technologically advanced setting, the primary catalysts for criticality accidents are often violations of established safety procedures and an insufficient safety culture. It highlights the indispensable role of administrative controls, rigorous operator training, and unwavering procedural adherence, all of which are directly applicable to the safe management of fuel in modern containers and storage pools.

While most criticality incidents have involved solutions, the event at the Siberian

Chemical Combine (Tomsk-7) on December 13, 1978, stands as an example of a criticality accident involving solid fissile material during handling operations [15]. Driven by production pressure and in direct violation of established protocols, two operators incorrectly loaded four plutonium metal ingots into a single storage container designed for only one. Although the container incorporated engineered safety features such as cadmium and polyethylene for shielding and interaction control, the primary safeguard was the administrative mass limit. As the fourth ingot was being placed, the configuration became prompt critical. The event was terminated by the thermal expansion and subsequent mechanical displacement of the ingots. One operator suffered a severe radiation dose that necessitated the amputation of both arms. Like the Tokai-mura incident, this event shows that human error and the disregard for mass and loading limits can override engineered safety measures. The lesson is directly transferable to the loading of fuel assemblies into containers, where procedural compliance is a critical layer of defense.

The risk posed by the slow, undetected accumulation of fissile material over extended periods is another crucial lesson derived from historical events. A 1997 accident at the Novosibirsk Chemical Concentration Plant was triggered by the gradual buildup of a uranium oxide slurry and crust at the bottom of two parallel slab tanks over many years. An investigation later revealed that the tanks' actual geometry was thicker than specified in their design and presented deformed regions, whose location was closely correlated with the location of the solid crust [15]. This event highlights a credible long-term hazard for spent fuel pools, i.e. the potential for slow degradation of fuel assemblies and the subsequent accumulation of fissile debris in an unanalysed geometry at the bottom of the pool. It underscores the necessity for conservative assumptions in safety analyses and for robust surveillance programs to monitor the long-term integrity of stored fuel.

2.6 Burnable Absorbers

Neutron absorbers are materials introduced into a system containing fissile material to control reactivity by capturing neutrons that would otherwise be available to cause fission. They are a fundamental tool for ensuring criticality safety out of the core and for optimizing the performance of the reactor core over its operational cycle. These absorbers can be employed in the FAs, in fixed structures or they can be dissolved in water. This section focuses on absorbers integrated in the FAs and in fixed structures, which are of particular relevance to this thesis.

Burnable Absorbers (BAs) are materials containing nuclides with large neutron absorption cross-sections (σ_a). They are typically placed in the reactor core as they reduce the excess of reactivity available in fresh fuel at the beginning of the cycle, allowing for the use of fuel with higher initial enrichment [17]. As the reactor operates, the BA material and the fuel both get depleted through neutron capture. Ideally, the BA burns out at a rate that compensates for the fuel's reactivity loss, helping to flatten the core's reactivity swing over the cycle and reduce the burden on control rods [17].

The effectiveness and burnout rate of a BA are highly dependent on its absorb-

ing isotopes and the local neutron energy spectrum. A key challenge in BAs design is managing self-shielding, where the outer layers of the absorber material shield the inner layers from the neutron flux. This phenomenon, which can be categorized as spatial self-shielding or energy self-shielding, causes the absorber to deplete non-uniformly and affects its overall worth throughout the cycle [17].

BAs can be incorporated into the core in several ways, but two common methods for commercial Light Water Reactors (LWRs) are as discrete burnable absorber rods or as integral absorbers mixed with or coated onto the fuel itself. Westinghouse currently integrates BAs in their FA production in the ways described in Subsection 2.6.1 and Subsection 2.6.2.

2.6.1 Integral Fuel Burnable Absorbers

One common method is to integrate the absorber directly with the fuel. An example is the Integral Fuel Burnable Absorber (IFBA) developed by Westinghouse, where fuel pellets are coated with a thin layer of zirconium diboride (ZrB_2) [17]. As shown in Figure 2, the ^{10}B isotope in the coating has a high thermal absorption cross-section and is depleted over the initial part of the fuel cycle. Because the absorber is a thin coating and not mixed with the fuel matrix, the helium produced from the $^{10}B(n, \alpha)\ ^{7}Li$ reaction has a less significant impact on the fuel's thermal conductivity or internal gas pressure compared to a homogeneously mixed absorber [17].

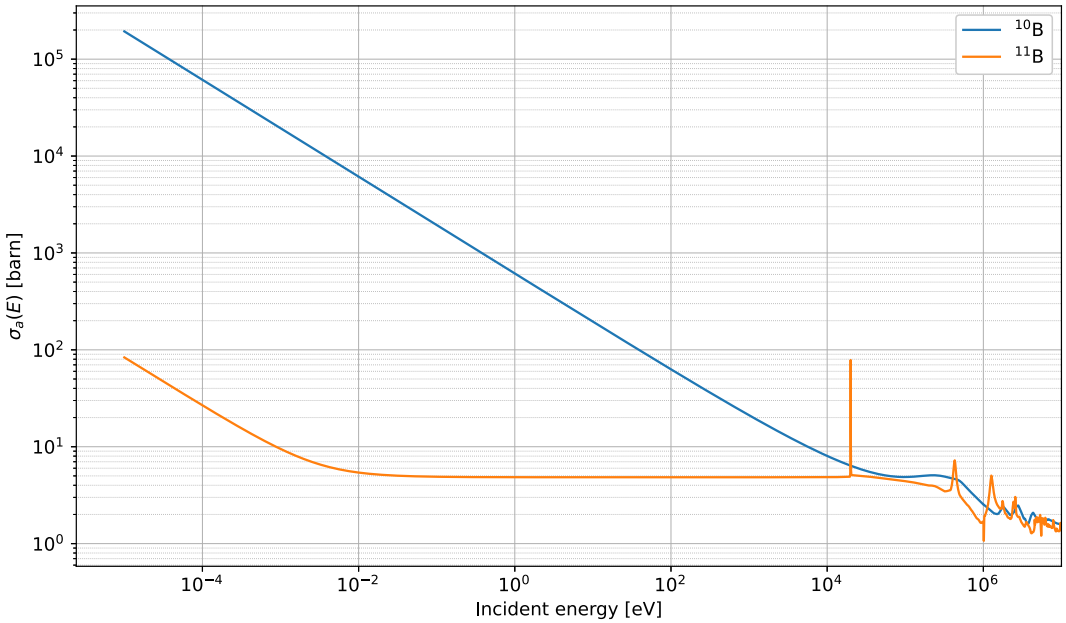

Figure 2: Neutron absorption cross sections for ^{10}B and ^{11}B as a function of incident neutron energy. Data obtained from the ENDF/B-VIII.0 library [12].

2.6.2 Gadolinium-Bearing Fuel Rods

Gadolinium is one of the most widely used burnable absorbers , typically employed as gadolinium oxide Gd_2O_3 homogeneously mixed with UO_2 powder during fuel pellet fabrication. It has an extremely high thermal neutron absorption cross-sections of two of its stable isotopes, $^{155}\mathrm{Gd}$ and $^{157}\mathrm{Gd}$, which are among the highest of any known nuclides [17].

This property makes gadolinium a ”black” absorber for thermal neutrons, meaning it is highly effective at compensating for excess reactivity. However, this same characteristic also leads to strong local flux depression and significant spatial self-shielding. Neutrons entering a gadolinium-bearing pellet are highly likely to be absorbed near the surface, shielding the interior of the pellet from the neutron flux. As a result, the gadolinium depletes in an ”onion-skin” fashion, burning out progressively from the outside in [17].

The primary challenge with gadolinium, and a central theme of this thesis, is its strong spectral sensitivity. Its odd mass number isotopes have absorption cross-section that are orders of magnitude higher at thermal energies than at epithermal or fast energies, as can be seen in Figure 3. A harder spectrum will render it less effective, while a softer, more thermalized spectrum will significantly increase its absorption worth. This behavior is the physical reason why reactivity equivalence methods based on in-core conditions can fail when applied to different, more moderated environments like storage containers or spent fuel pools.

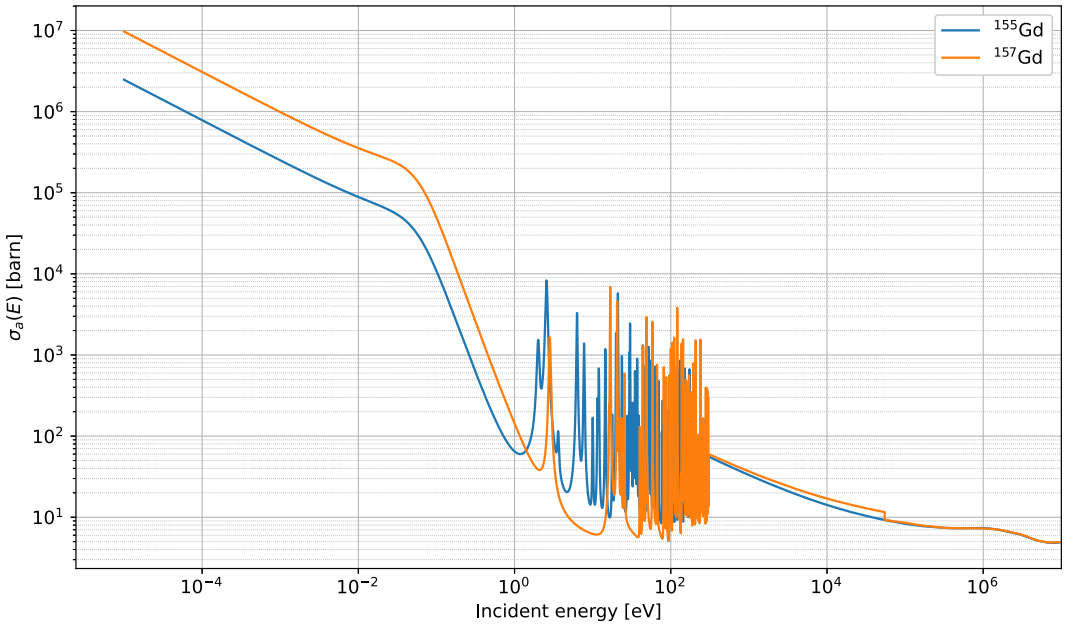

Figure 3: Neutron absorption cross sections for $^{155}\mathrm{Gd}$, and $^{157}\mathrm{Gd}$ as a function of incident neutron energy. Data obtained from the ENDF/B-VIII.0 library [12].

2.7 The Reactivity Equivalence Method

The most commonly employed approach for licensing storage infrastructures for fuel with higher $^{235}\mathrm{U}$ enrichment and BAs relies on explicit three-dimensional modeling, which can be computationally demanding. As an alternative, the nuclear industry has long explored reactivity equivalence relations that relate irradiated or higher-enrichment fuel with burnable absorbers to standard reference fuels.

The Reactivity Equivalence Method is a comparative approach often employed in criticality safety analyses to justify the introduction of fuel with higher enrichment into a system, such as a storage container or rack, that was originally licensed for a lower enrichment. The fundamental principle is to demonstrate that a fuel assembly with a higher enrichment but containing a specific arrangement of burnable absorbers (e.g., gadolinium rods) is at least as safe as, or less reactive than, a reference fuel assembly at the maximum licensed enrichment without any burnable absorbers.

This methodology effectively mirrors the regulatory practice of establishing a reactivity threshold based on a Standard Cold Core Geometry (SCCG) without gadolinium credit, a concept formalized in technical bases such as NUREG/CR-7194 [1]. In this framework, the reference fuel configuration (at maximum licensed enrichment but without absorbers) defines the bounding reactivity limit for the system within a reference core environment. This method allows for flexibility in what kind of FAs can be safely stored as their actual characteristics can be taken into account.

Typically, this equivalence is established by comparing the infinite multiplication factor (k_∞) of both configurations in a reference geometry, which is often representative of the tightly-packed, relatively under-moderated conditions of a reactor core. If the k_∞ of the new fuel (higher enrichment with absorbers) is shown to be lower than or equal to that of the reference fuel, the two are considered reactively equivalent, and the new fuel is deemed acceptable for storage.

However, a critical underlying assumption of this method is that the neutronic behavior of the two fuel types will scale similarly when they are moved from the reference geometry (the core) to the actual storage geometry (the container or spent fuel pool). Therefore, the adequacy of transferring these equivalence relations across different geometries has been questioned.

3 Methodology

This chapter presents the methodology developed to assess the validity of the Reactivity Equivalence Method. It begins by defining the key physical components used in the analysis: the Reference Fuel Assembly Design (Section 3.1), the Fresh Fuel Container Design (Section 3.2), and the SFP Design (Section 3.3). Next, the idealized Core Reference Configuration (Section 3.4) is described, which serves as the basis for establishing the equivalence threshold. After introducing the geometric definitions, the Modeling Approach (Section 3.5) is outlined, including the computational tool MCNP, the general and specific modeling assumptions, and the criteria used to determine absorber distributions. The chapter concludes with the formal five-step Reactivity Equivalence Evaluation procedure (Section 3.6), which underpins all subsequent analyses presented in this thesis.

3.1 Reference Fuel Assembly Design

In this thesis, all the criticality analyses were performed using the Westinghouse VVER-1000 RWFA design developed for the Temelín Nuclear Power Plant in the Czech Republic [18]. Hereafter, this reference design will be referred to as RWFA-T. Unlike other LWRs, the VVER-1000 core is loaded with hexagonal FAs. Table 1 lists the key design parameters for the RWFA-T model, extracted from the official specification sheet [18]. Additional design specifications and material compositions are proprietary to Westinghouse Electric Company and cannot be disclosed in this work.

Table 1: Key Design Parameters of the RWFA-T [18]

Parameter	**Value**
Number of Fuel Rods	312
Number of Guide Tubes	18
Number of Instrument Tubes	1
Fuel Rod Pitch	12.75 mm
Pellet Diameter	7.844 mm
Fuel Rod Inner Diameter	8.001 mm
Fuel Rod Outer Diameter	9.144 mm
Active Fuel Stack Length	3650 mm
Cladding Material	Optimized ZIRLO™
Guide & Instrument Tube Material	ZIRLO™

3.2 Fresh Fuel Container Design Description

The first of the two physical configurations modeled for evaluating the applicability of the Reactivity Equivalence Method to criticality analysis is the fresh fuel container. The specific container design employed at the Temelín Nuclear Power Plant was used for the analysis to maintain consistency with the reference fuel. Under normal conditions, the container is dry and designed to hold 18 FAs, which are arranged in a hexagonal lattice with a significantly larger lattice pitch compared to that of the reactor core. The fresh fuel container geometry is fully described in [19]. The report also analyses the maximum $^{235}\mathrm{U}$ enrichment for fuel without burnable absorbers that can be safely stored in this container.

3.3 SFP Design Description

The second physical configuration modeled for the criticality analysis is the SFP. The design was based on the storage facility at the Temelín Nuclear Power Plant to maintain consistency with the fuel assembly choice. The SFP geometry is fully described in [19]. After being unloaded from the reactor, the fuel assemblies are not housed within a container but are instead directly immersed in the pool, as they require active cooling. Each storage position consists of a rack cell, which forms a cage made of borated stainless steel. The reactivity of the fuel was analysed in a similar environment to investigate the non-additive, competitive effects between the two different types of absorbers present: gadolinium within the fuel rods and boron in the external racks. This analysis primarily aims to demonstrate the limitations of simplified reactivity equivalence methods when applied to such complex spectral environments.

3.4 Core Reference Configuration

The core reference configuration models the VVER-1000 RWFA-T fuel assembly in an infinite hexagonal lattice with a pitch representative of an in-core environment. This configuration is not intended to represent a physical storage condition; rather, its purpose is to be used to calculate the infinite multiplication factor (k_∞) under the tightly-packed, harder-spectrum conditions typically used to establish the reactivity equivalence criterion in industrial practice.

3.5 Modeling approach

3.5.1 Computational Tool: Monte Carlo N-Particle Transport Code

All the criticality analyses in this work were conducted using the MCNP code, version 6.2, developed at Los Alamos National Laboratory [4]. MCNP is a general-purpose, continuous-energy Monte Carlo transport code widely used for applications including criticality safety, shielding, and reactor physics. Its ability to model complex three-dimensional geometries with high fidelity makes it an industry-

standard tool for safety and licensing analyses. The computational methodology implemented in MCNP was validated by the code developers at Los Alamos National Laboratory [20]. In addition, Westinghouse performed an extensive validation of the specific combination of cross-section libraries and the MCNP code used for criticality safety analyses, benchmarking the results against a comprehensive experimental dataset, as documented in [21, 22]. While this validation process establishes a calculational bias, its absolute value is not a primary concern for the present work. Since this thesis is fundamentally a comparative analysis, aimed at understanding when the Reactivity Equivalence Method is applicable, it focuses on the relative differences between calculated results. It is therefore assumed that the bias affects all configurations systematically, and the conclusions drawn from comparing k_{eff} values remain valid.

MCNP employs the `KCODE` card to calculate the k_{eff} of the system by simulating the life of individual neutrons. Unlike deterministic methods that solve the Boltzmann transport equation for average particle behavior, MCNP tracks each neutron from its birth (e.g., from fission) through its life to its eventual death (by absorption or leakage). The interaction of the neutron with matter is determined by randomly sampling probability distributions based on continuous-energy nuclear cross-section data. Unlike fixed-source problems where particles are tracked from a defined source until they are absorbed or escape, criticality calculations involve a dynamic source that evolves over successive generations, or cycles, of neutrons.

The simulation begins with an initial guess for the spatial distribution of fission source points. During the random walk of neutrons in a cycle, the code estimates the number of fission neutrons that would be produced in the next generation based on the collisions occurring in the current generation. The locations of these new fission sites are stored to serve as the source points for the subsequent cycle. This iterative process continues over many cycles to allow the fission source distribution to converge to the fundamental eigenmode of the system. To ensure the accuracy of the final result, the initial cycles before convergence is achieved are discarded as inactive cycles. Once the source distribution has converged, the active cycles begin, and statistical data collection commences to calculate the effective multiplication factor.

MCNP computes k_{eff} using a statistical combination of three independent estimators. The *collision estimator* evaluates k_{eff} from the expected number of fission neutrons produced at sampled collision sites. The *absorption estimator* is based on the number of neutrons absorbed in fissile nuclides, utilizing analog or implicit absorption sampling. The *track-length estimator* infers fission production by integrating the neutron flux, represented by particle track lengths, through fissionable materials. A detailed discussion of the formulation and implementation of these estimators can be found in [23]. For the final result, MCNP performs a statistical combination of these estimates averaged over the active cycles to produce a mean k_{eff} and a standard deviation. The Halperin algorithm, which combines the results obtained with all three estimators, gives the best final estimate from an MCNP calculation, even when the true value lies outside of the range. [23]

For each simulation, multiple key simulation parameters, such as the number of neutron histories per cycle, the number of inactive cycles, and the number of active cycles, were carefully selected. The values employed for each geometric configuration are detailed in Table 2. The main objective was to achieve a standard deviation on the final k_{eff} value that was sufficiently small to ensure that the reactivity differences between various configurations were statistically significant and not due to random fluctuations. Furthermore, the number of active cycles was chosen to be large enough for the calculated k_{eff} values to appear normally distributed at the 95% confidence level, as verified by the statistical checks provided as an output by MCNP. Throughout this thesis, all error bars shown in plots represent this 95% CI (Confidence Interval), which is derived from the final standard deviation (σ) of the converged k_{eff} calculation.

Table 2: MCNP simulation parameters selected for each geometric configuration

Configuration	Histories per Cycle	Inactive Cycles	Active Cycles
Core Geometry	5×10^4	20	130
Fresh Fuel Container	5×10^4	100	100
Spent Fuel Pool (SFP)	5×10^4	130	500

In addition to the k_{eff} calculations, neutron flux tallies (MCNP card `F4`) were defined with a detailed energy bin structure (card `E4`) at key locations. These tallies were defined to quantify and compare the neutron energy spectrum across the different geometries, providing the physical data required for the interpretation of the reactivity results in Chapter 5. Table 3 defines these tally locations, which will be referred to throughout Chapter 4 and Chapter 5. Moreover, since the source definition differs between these models, the absolute flux magnitude is not directly comparable. Therefore, all spectra within a single simulation are normalized by the single maximum flux value found across all tallies in that specific simulation. This method preserves the relative flux magnitude differences between spatial locations while allowing the spectral shapes of different geometries to be compared.

Table 3: Description of tally locations used in the MCNP spectral analysis

Location	**Description**
A	Moderator surrounding a fuel pin in the outermost ring of the fuel assembly
B	Moderator near the central guide tube
C	Moderator adjacent to a gadolinium-bearing fuel rod
D	Moderator in the water gap between the fuel assembly and the borated steel rack in the SFP model

The choice of a Monte Carlo method over a deterministic approach was driven by the geometric complexity of the systems under investigation. The heterogeneous arrangements of fuel rods, guide tubes, structural materials, and absorbers within the fuel assemblies and storage racks are challenging to represent accurately with the spatial, angular, and energy group approximations inherent to

most deterministic solvers. MCNP's ability to model these complex 3D geometries without significant geometric simplification or energy homogenization ensures a high-fidelity representation of the physical reality, which is crucial for obtaining reliable and conservative results in criticality safety assessments.

3.5.2 General Modeling Assumptions

To ensure that the results of a criticality safety analysis are robust and conservative, a series of bounding assumptions were applied to the simulation models. This approach is designed to systematically account for uncertainties in physical parameters, manufacturing tolerances, and potential off-normal conditions, ensuring that the calculated k_{eff} represents a conservative upper bound of the system's true reactivity. The following general assumptions were applied consistently across all geometric configurations analysed in this work, unless specified otherwise.

- All fissile materials were modeled assuming the same pin enrichment over the entire active fuel length, and no credit was taken for any natural enrichment axial blankets.
- No credit is taken for any spacer grids or spacer sleeves.
- Manufacturing tolerances for geometric parameters, such as pellet diameter and cladding thickness, were chosen to maximize system reactivity. Non-structural components with negligible neutronic impact were omitted from the models. Conversely, any structural materials located between fissile units and neutron absorbers were explicitly modeled to conservatively account for their neutron scattering effects.
- The moderator, when present, is always modelled as pure water, without any boron dissolved in it.
- All materials were modeled at a standard ambient temperature of $293\,\mathrm{K}$. This is considered the most reactive condition for the under-moderated or optimally moderated thermal systems under investigation.

Specific assumptions unique to each of the modeled geometries are detailed in the following Section.

3.5.3 Specific Model Implementations

The core reference model was designed to calculate the k_{∞} under conditions representative of an in-core environment. The model consists of a fuel assembly within a hexagonal lattice that is infinite in the lateral extent but finite axially, as Monte Carlo simulations require explicit three-dimensional geometries. To simulate an infinitely repeated array, reflective boundary conditions were applied to all six lateral faces as well as the top and bottom surfaces.

For the fresh fuel container configuration, a parametric study was performed by varying the water density under fully flooded conditions to identify the point of *optimal moderation*, i.e. the state that yields the highest possible k_{eff}. This bounding approach ensures the system is assessed at its most reactive moderation state. Furthermore, to ensure maximum neutron reflection, the model was enclosed by a full-density water reflector of at least $30\,\text{cm}$. A concrete base was also included below the container to conservatively account for neutron reflection from the ground or supporting structures.

As regards the SFP, its configuration was simplified to a unit cell representing a single storage rack position. In this model, a fuel assembly is surrounded by its borated stainless steel cage and immersed in water. To simulate the large, repeating array of a full storage rack, periodic boundary conditions were applied to the lateral borders of the unit cell. This technique effectively models an infinite lattice of identical fuel assemblies. It also allows for an accurate calculation of the multiplication factor in a SFP environment while significantly reducing the computational complexity of a full-pool simulation. Furthermore, the FA is modeled at its most reactive point in life, which was determined to be at the beginning of life, including the cases in which the FA include Gd-bearing rods [24].

3.5.4 Absorber Distributions

For each fuel enrichment higher than the maximum allowed without BA, different gadolinium rod patterns were analysed to identify the configuration associated with the maximum system reactivity, thereby ensuring a conservative assessment of the equivalence method. The placement of these absorber rods is subject to specific design restrictions intended to prevent excessive local power depression. Specifically, gadolinium rods are not permitted in the two outermost rows of the fuel assembly or in positions adjacent to the guide tubes, as these locations are characterized by a higher degree of water moderation which would result in an undesirably high reactivity worth for the absorber.

To systematically identify all unique placement patterns satisfying these constraints, the rotational symmetry of the FA was exploited. By applying the restrictions within this symmetry sector, the complete set of distinct permissible locations for gadolinium rod placement was determined. These locations formed the basis for generating the different configurations analysed in this study.

3.6 Reactivity Equivalence Evaluation

The Reactivity Equivalence Method is a common licensing approach that relies on comparing the infinite lattice multiplication factor (k_∞) of gadolinium-bearing fuel with that of a reference fresh fuel at maximum allowable enrichment without absorbers. In this work, k_∞ values were obtained from the core reference geometry, while k_{eff} values were computed for the full 3D container and spent fuel pool configurations. Discrepancies in the scaling of these values provide insight into the limitations of using in-core equivalence to justify storage of higher-enrichment

fuel in different neutron environments.

To systematically test the Reactivity Equivalence Method, the following procedure was applied for each configuration (e.g., 3 and 6 gadolinium rods).

- Firstly, the reference infinite multiplication factor in core geometry $k_{\infty,\text{ref}}$ has to be established. To do so, the maximum enrichment for fuel without burnable absorbers is progressively increased in full 3D container geometry to identify the maximum enrichment for fuel without burnable absorbers that meets the safety limit ($k_{\text{eff}} \leq 0.95$). The corresponding k_∞ for this reference fuel was then calculated in the core reference geometry to establish the threshold for equivalence.
- Secondly, based on the FA's symmetry and the placement restrictions detailed in Subsection 3.5.4, all unique and permissible lattice positions for placing the gadolinium-bearing rods were identified.
- For a given number of gadolinium-bearing rods, the fuel enrichment was then increased until its k_∞ in the core reference geometry matched $k_{\infty,\text{ref}}$.
- To keep the analysis conservative, the gadolinium rod pattern that produced the highest reactivity (i.e., the most conservative or least effective arrangement) has to be identified, in this case using the core reference geometry.
- The equivalent configuration from the previous steps (with the determined enrichment and most reactive rod pattern) was then simulated in the full 3D container or SFP geometry to calculate its actual k_{eff}. This value was then compared against the k_{eff} obtained in the same conditions for the reference case to assess the validity of the equivalence method.

4 Results

This chapter presents the numerical results obtained from the MCNP 6.2 simulations. The analysis is structured following the procedure described in Section 3.6.

4.1 The Reference Case

The first step of the analysis was to establish a conservative reference case for fuel without any BA. Multiple criticality simulations with decreasing enrichment from an initial guess value were performed to identify the maximum enrichment that yielded a compliant k_{eff} value in the fresh fuel container. This enrichment level will hereafter be referred to as ϵ_{ref}.

A parametric study on fuel with ϵ_{ref} was conducted by varying the density of the water moderator from $0.1\,\text{g/cm}^3$ to $1\,\text{g/cm}^3$ to identify the condition of *optimum moderation*. Figure 4 shows the results of such analysis, and the highest reactivity for the container configuration occurs at a water density of 0.2 g/cm^3. This peak reactivity, which does not include corrections for calculational bias or uncertainties, was confirmed to be below the safety limit of 0.98. In nominal conditions, i.e. when the container is not flooded, the system yields $k_{\text{eff}} = 0.19362$ with standard deviation $\sigma = 0.00010$. In the spent fuel pool configuration the system yields $k_{\text{eff}} = 0.93488$ with $\sigma = 0.00011$.

This safe reference configuration yields $k_{\infty} = 1.45966$ with $\sigma = 0.00030$ in core geometry. This value is hereafter referred to as $k_{\infty,\text{ref}}$, serving as the reactivity equivalence threshold for the subsequent analyses.

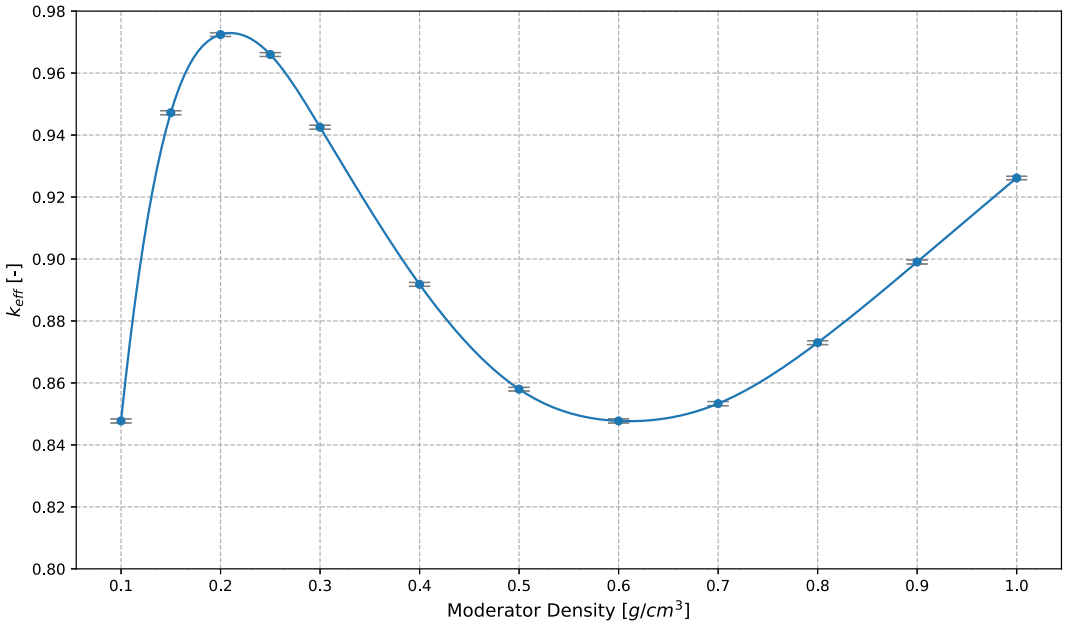

Figure 4: Effect of water moderator density on k_{eff} for the reference fuel in the fresh fuel container geometry, identifying the optimal moderation point. Error bars represent the 95% CI.

4.2 Permissible Gadolinium Rod Locations

Applying the placement restrictions and symmetry considerations detailed in the methodology (Subsection 3.5.4), the set of unique, permissible lattice positions for Gd-bearing rods was determined within the FA symmetry sector. Figure 5 illustrates and labels these allowed locations.

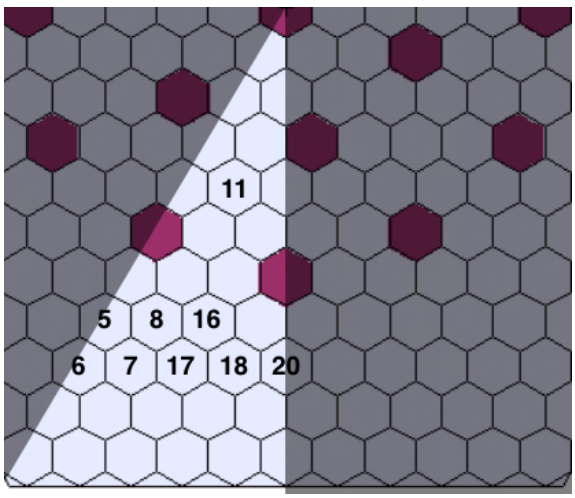

Figure 5: Map showing the permissible and uniquely labeled lattice positions for gadolinium-bearing rods within a sector of the FA.

4.3 Fresh Fuel Container Analysis

Following the establishment of the reference case, the Reactivity Equivalence Method was tested in the fresh fuel container for fuel assemblies containing 3 and 6 gadolinium-bearing rods. The gadolinium-bearing rods have the same $^{235}\mathrm{U}$ enrichment as the non-gadolinium-bearing rods and have ϵ gadolinium content.

4.3.1 Case with 3 Gadolinium Rods

For the configuration with three gadolinium rods, the fuel enrichment was increased until its k_∞ calculated in the core reference geometry matched the established threshold, $k_{\infty,\text{ref}}$. Based on the permissible Gd rod locations identified in Figure 5, all symmetric arrangements were considered for placing three gadolinium rods to identify the pattern that yields the highest reactivity. The specific configurations investigated are shown in Figure 6.

Using the core geometry, the maximum $^{235}\mathrm{U}$ enrichment that yields a k_∞ that still satisfies $k_\infty < k_{\infty,\text{ref}}$ was determined using the configuration with gadolinium rods in position 11 (Figure 6e). Through iterative calculations, this required enrichment was found to be $1.12 \times \epsilon_{\text{ref}}$. This enrichment value was then used for simulating all other symmetric 3-rod patterns.

The calculated k_∞ for each of the identified symmetric 3-Gd-rod arrangements in the core reference geometry is presented in Figure 7. All the configurations yield $k_\infty < k_{\infty,\text{ref}}$. As shown, the configuration with gadolinium rods placed in position 7 (Figure 6c) yielded the highest k_∞ value. This pattern represents the least effective placement of the burnable absorber within the assessed configurations under these spectral conditions. Therefore, to ensure a conservative analysis according to the procedure outlined in Section 3.6, this specific rod arrangement and its corresponding fuel enrichment were selected as the *equivalent* configuration for the subsequent criticality assessment in the full 3D container geometry.

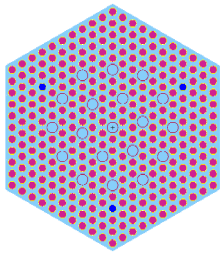

(a) Position 5.

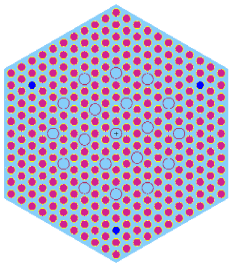

(b) Position 6.

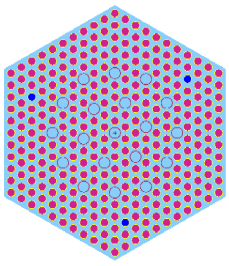

(c) Rods in pos. 7.

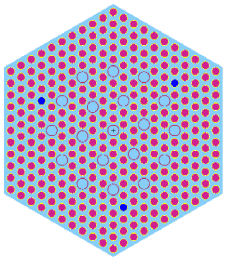

(d) Position 8.

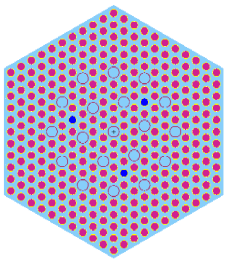

(e) Position 11.

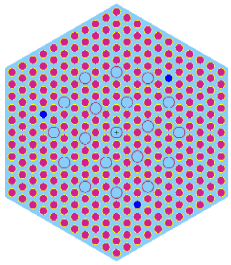

(f) Position 16.

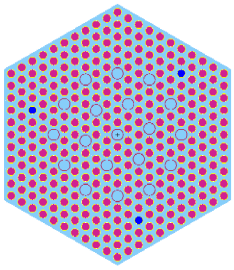

(g) Position 17.

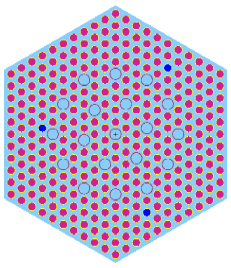

(h) Position 18.

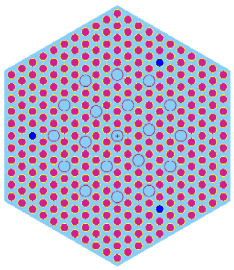

(i) Position 20.

Figure 6: Investigated placement patterns for three gadolinium-bearing rods. Gadolinium-bearing rods are depicted with blue circles.

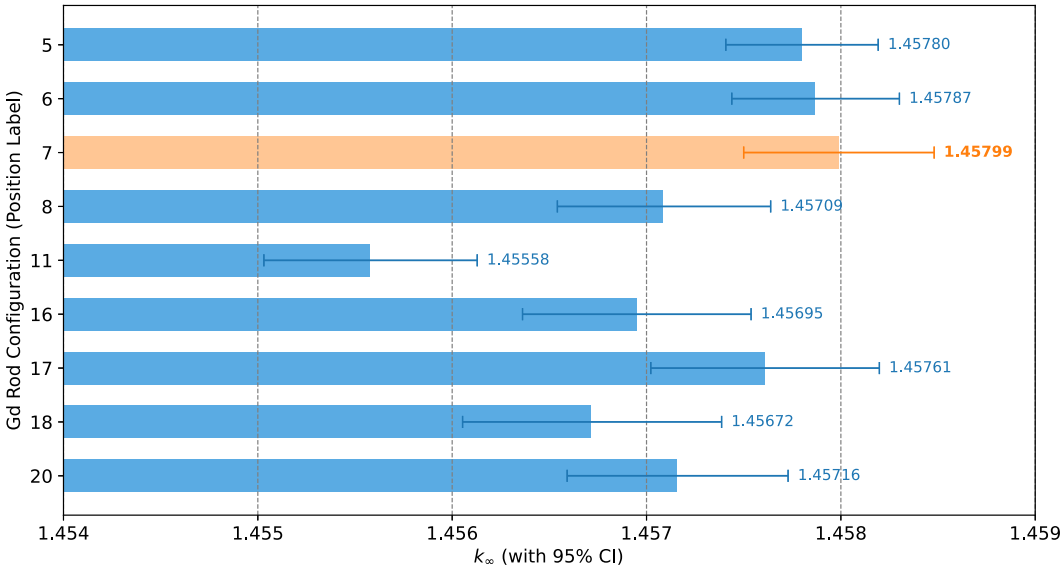

Figure 7: k_∞ for various 3-Gd-rod configurations simulated in the core reference geometry. The configuration yielding the highest reactivity is highlighted. Error bars indicate the 95% CI.

The resulting *equivalent* fuel assembly was then simulated in the full 3D container geometry with different moderator densities. As shown in Figure 8, the results demonstrate a clear failure of the Reactivity Equivalence Method. The results in the container show the gadolinium-bearing assembly to be consistently more reactive than the reference case across the entire range of moderator densities examined, including both the optimal moderation point and full-density flooding conditions. This finding contradicts the fundamental assumption of the Reactivity Equivalence Method based on k_∞.

4.3.2 Case with 6 Gadolinium Rods

The analysis procedure was repeated for configurations containing six gadolinium-bearing rods. For this case, the maximum allowable fuel enrichment was used, denoted as ϵ_{max} (where $\epsilon_{\text{max}} > 1.12 \times \epsilon_{\text{ref}}$), determined by safety constraints in the manufacturing process. Initial calculations in the core reference geometry confirmed that even with this higher enrichment, the k_∞ values for the evaluated 6-rod patterns remained below the established threshold, $k_{\infty,\text{ref}}$.

To identify the most reactive (least effective) placement for six rods, several patterns were investigated (Figure 9). The selection of these patterns was guided by the results from the 3-rod analysis, focusing on combinations involving the individually most reactive positions (5, 6, and 7), as well as configurations incorporating rods near the center of the assembly (position 11) and mixed inner/outer arrangements (positions 5 and 11) to explore different spatial distributions.

The calculated k_∞ values for these 6-rod configurations using enrichment ϵ_{max} are presented in Figure 10. The pattern with rods placed symmetrically in position 7 (as shown in Figure 9c) yielded the highest k_∞, confirming it as the least effective

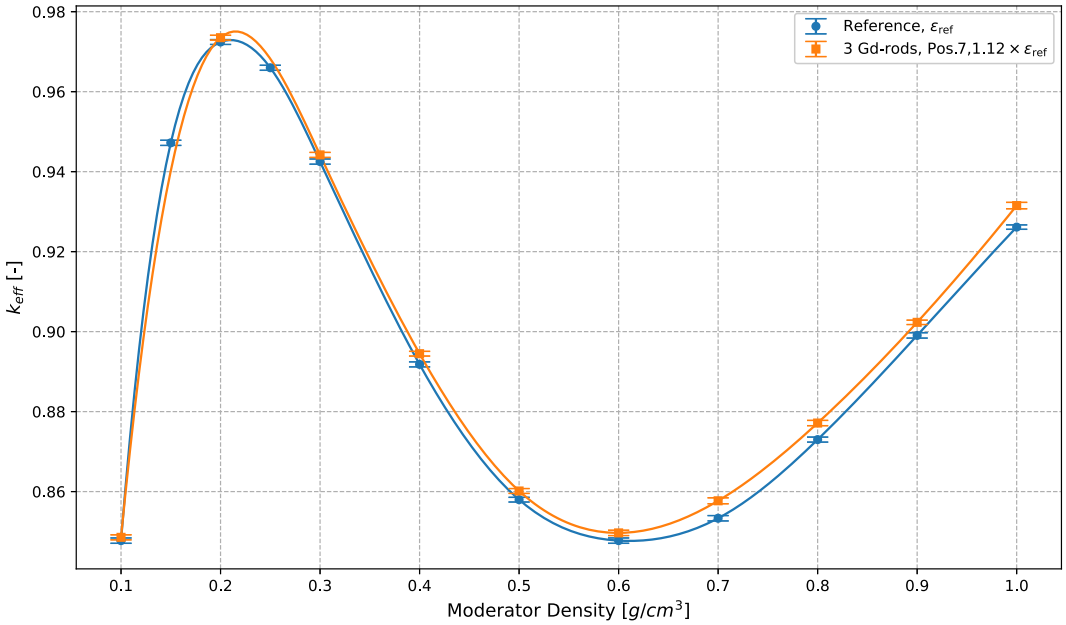

Figure 8: Effect of water moderator density on k_{eff} for the reference fuel and the fuel with 3 Gd rods in position 7 with $^{235}\mathrm{U}$ enrichment equal to $1.12 \times \epsilon_{\text{ref}}$ in the fresh fuel container geometry. Error bars represent the 95% CI.

arrangement among those tested under core spectrum conditions.

This *equivalent* 6-Gd-rods fuel assembly (position 7 pattern, enrichment $\epsilon_{\max}$) was then simulated in the full 3D container geometry across the range of moderator densities. The results, compared against the reference case in Figure 11, further confirm the failure of the Reactivity Equivalence Method. Similar to the 3-rod case, the 6-rod gadolinium-bearing assembly exhibited consistently higher reactivity than the reference assembly at equivalent moderator densities, despite its k_∞ being below the reference threshold in the core geometry.

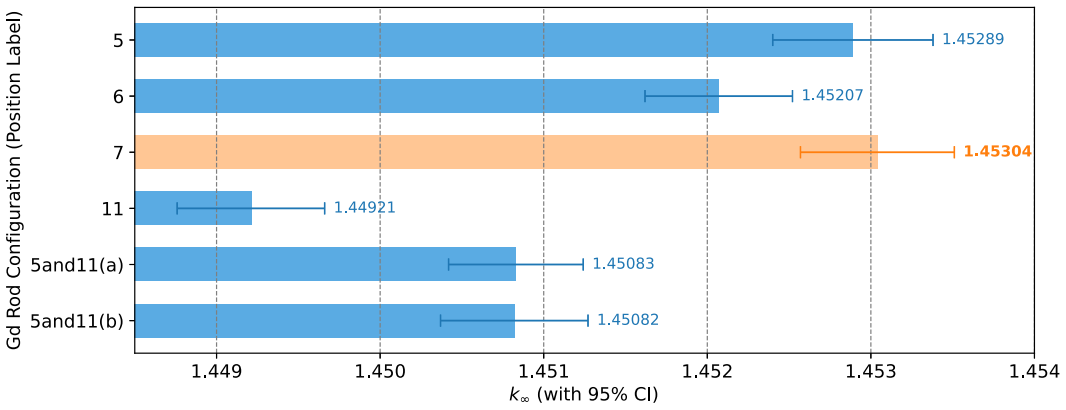

Figure 10: k_∞ for various 6-Gd-rod configurations simulated in the core reference geometry. The configuration yielding the highest reactivity (most conservative case) is highlighted. Error bars indicate the 95% CI.

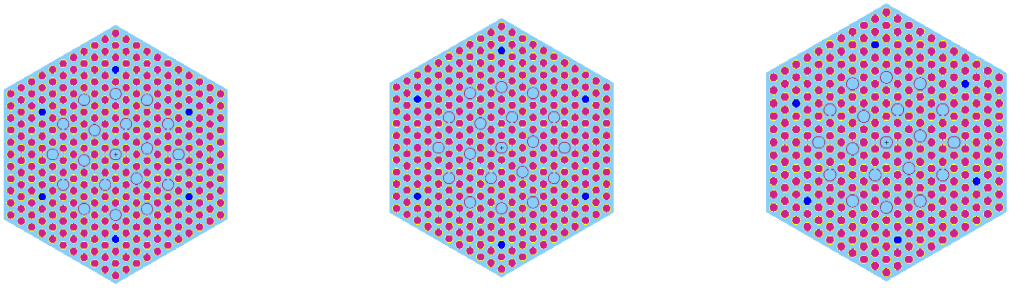

(a) Position 5. (b) Position 6. (c) Rods in pos. 7.

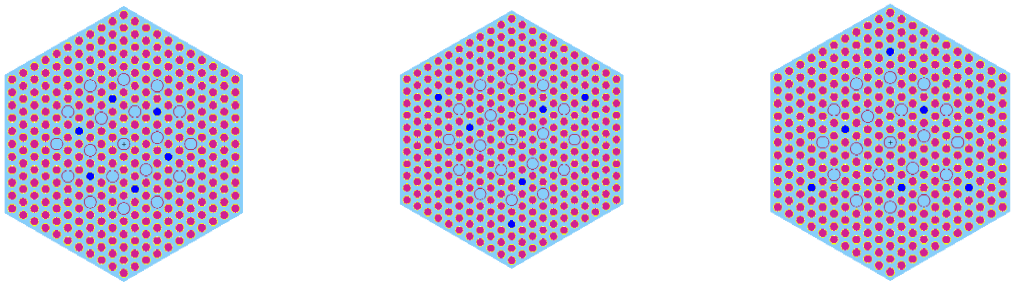

(d) Position 11. (e) Position 5 and 11, a. (f) Position 5 and 11, b.

Figure 9: Investigated placement patterns for six gadolinium-bearing rods. Gadolinium-bearing rods are represented with blue circles.

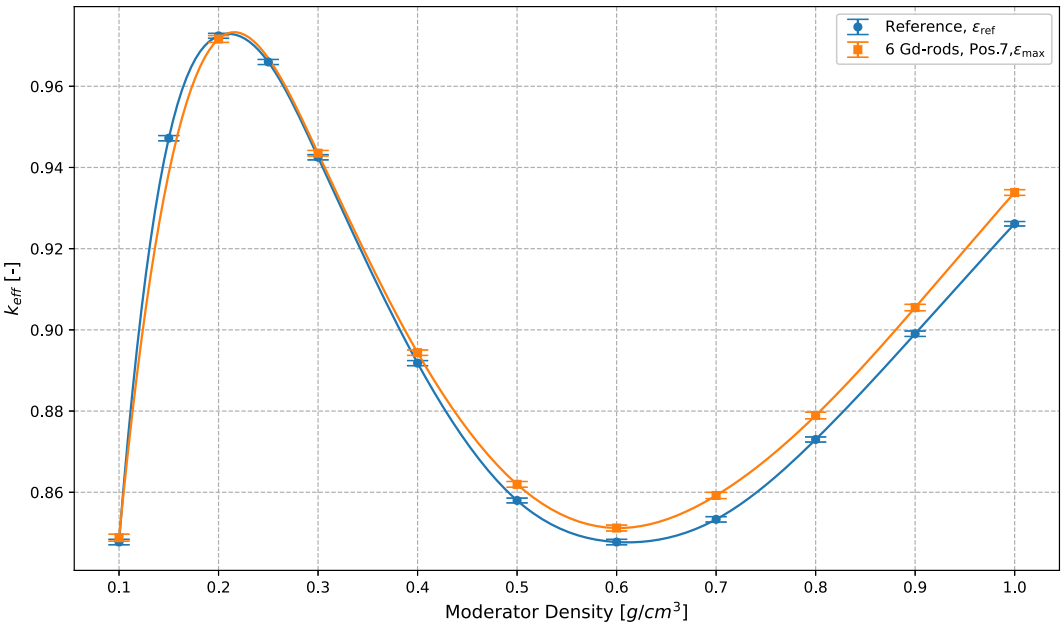

Figure 11: Effect of water moderator density on k_{eff} for the reference fuel and the fuel with 6 Gd rods in position 7 with ^{235}U enrichment equal to ϵ_{max} in the fresh fuel container geometry. Error bars represent the 95% CI.

4.3.3 Inconsistency of the Most Reactive Absorber Configuration

A key finding from the analysis is that the gadolinium rod pattern identified as the most reactive in the core reference geometry does not correspond to the most reactive pattern in the full 3D canister geometry. As illustrated in Figure 12, the reactivity ranking of configurations changes when moving from the core environment to the container environment. Specifically, the pattern that was most reactive in the core was among the least reactive in the container, while the most reactive pattern in the container (Position 11, $k_{\text{eff}} = 0.98387 \pm 0.00010$) was the least reactive in the core geometry. This result highlights that the simplified core model is not only non-conservative but also unreliable for identifying the actual worst-case absorber configuration in the storage scenario.

4.4 Spent Fuel Pool Analysis

Finally, the Reactivity Equivalence Method was evaluated for a SFP configuration, where the fuel assembly is surrounded by borated stainless steel storage racks (cells). The reference model (Section 4.1) was again used as the basis. The results of this analysis are summarized in Table 4. The table directly compares the k_{∞} for each case (calculated in the core geometry) with the resulting k_{eff} (calculated in the SFP geometry, for full-density water).

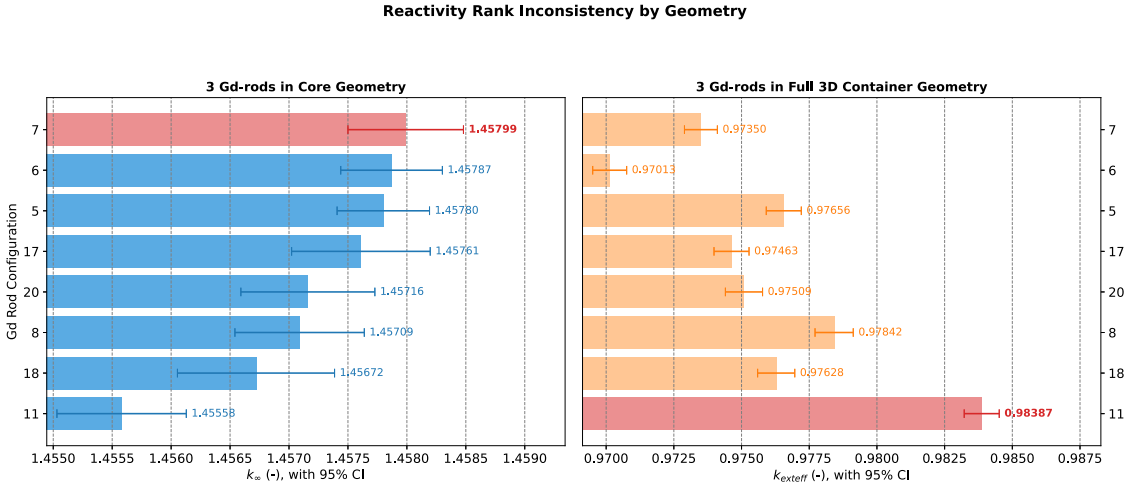

Figure 12: Side-by-side comparison of k_∞ (left, Core Geometry) and k_{eff} (right, 3D container Geometry) for the 3-rod Gd configurations. The y-axis is sorted by the reactivity rank of the core geometry. The bar highlighted in red indicates the most reactive configuration in each respective plot. The misalignment of the red bars visually confirms that the reactivity ranking is not consistent between the two models. Error bars show the 95% CI.

Table 4: Comparison of multiplication factors k_∞ (Core) and k_{eff} (SFP) for the reference and *equivalent* configurations

Case	**Core Geometry**		**SFP Geometry**	
	k_∞	σ_{k_∞}	$k_{\mathbf{eff}}$	$\sigma_{k_{\mathbf{eff}}}$
Reference (No Gd, ϵ_{ref})	1.45966	0.00030	0.93488	0.00011
3 Gd Rods (Pos. 7, $1.12 \times \epsilon_{\text{ref}}$)	1.45799	0.00025	0.94329	0.00011
6 Gd Rods (Pos. 7, $\epsilon_{\max}$)	1.45304	0.00024	0.94745	0.00011

The results confirm the failures observed in the fresh fuel container analysis, demonstrating once again that the method is non-conservative. Although the k_∞ values for the configurations containing gadolinium-bearing rods are lower than the reference, their k_{eff} values in the SFP geometry are significantly higher.

The 6-Gd-rod case, for example, has the lowest k_∞ in the core (1.45304) but produces the highest k_{eff} in the pool (0.94745). This represents a reactivity increase of $\approx$ 1257 pcm compared to the reference case (0.93488), eroding a substantial portion of the safety margin, even though the regulatory limit of 0.95 was not exceeded in this specific simulation.

4.5 Neutronic Spectrum Analysis

To acquire the data necessary to interpret the results presented in this Chapter, a detailed neutronic analysis was performed. This section presents the neutron flux spectra at the key locations defined in Table 3. As detailed in Subsection 3.5.1, all spectra are normalized to facilitate the comparison of spectral shapes. First, the spectra in the models without Gd are compared to establish the baseline neutronic

environments.

4.5.1 Spectral Comparison of Geometries (No Gd Cases)

Figure 13, Figure 14, and Figure 15 show the neutron flux spectra for the core, container, and SFP models in the reference configuration without Gd. Figure 13 reveals that the thermal neutron flux is relatively flat across the moderator regions (Location A and Location B).

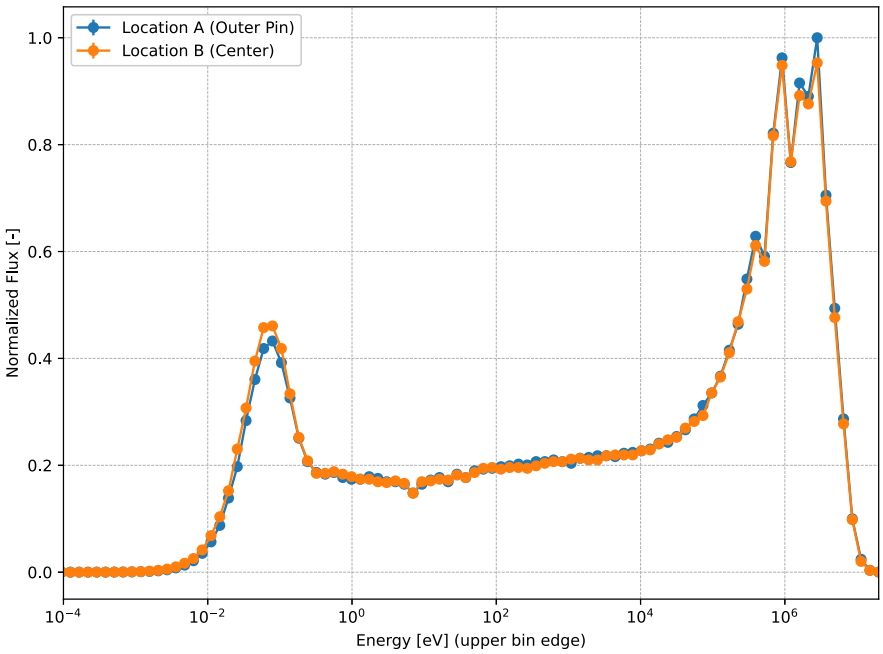

Figure 13: Neutron flux spectrum for the reference configuration without Gd in the core model. Curves correspond to tally locations in Table 3 and are normalized according to the procedure described in Subsection 3.5.1.

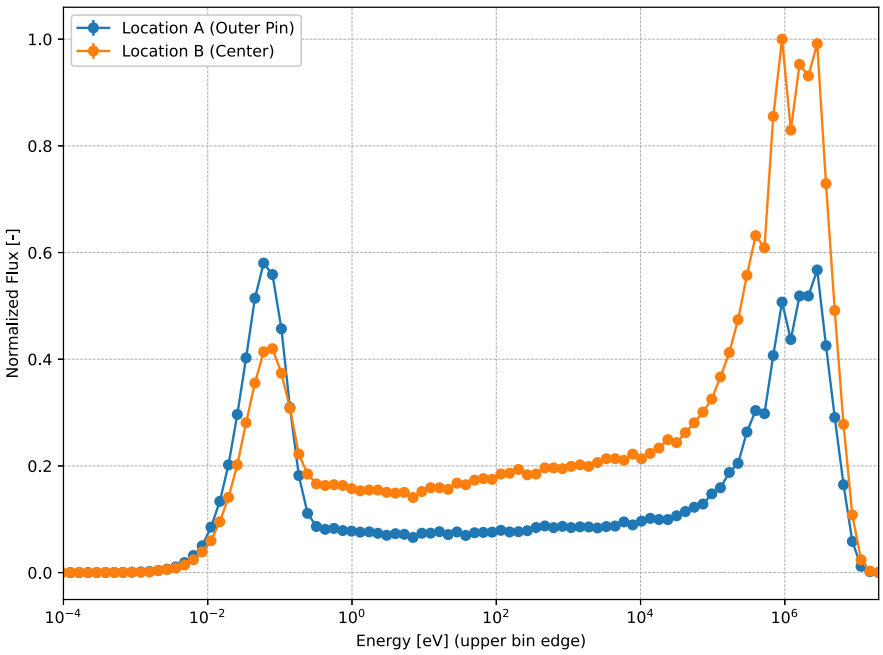

Figure 14: Neutron flux spectrum for the reference configuration without Gd in the container model. Curves correspond to tally locations in Table 3 and are normalized according to the procedure described in Subsection 3.5.1.

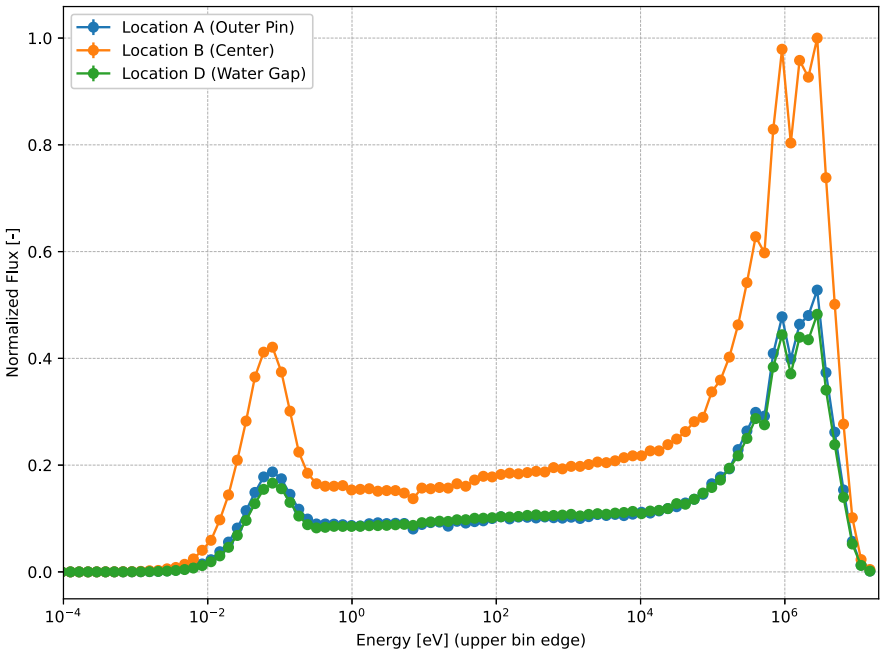

Figure 15: Neutron flux spectrum for the reference configuration without Gd in the SFP model. Curves correspond to tally locations in Table 3 and are normalized according to the procedure described in Subsection 3.5.1.

4.5.2 Effect of Gadolinium on Local Spectrum (3 Gd Rod Cases)

The spectra for the 3-Gd-rod cases were also analysed to observe the local effect of the BA. The following figures present the normalized flux spectra for the RWFA-T with Gd-bearing rods in Position 11 and Position 7, as in Figure 6e and Figure 6c, respectively. These configurations correspond to those identified in Figure 7 as being the least and most reactive in the core model, respectively, and which subsequently inverted their reactivity ranking in the container model, as shown in Figure 12.

The data in Figure 16, Figure 17, Figure 18, and Figure 19 shows the effect of the gadolinium rods on the local flux, in addition to the neutron spectrum at the center and in the periphery of the fuel assembly. Moreover, Figure 20 shows the neutron flux spectrum in the SFP model. This set of detailed spectral data provides the necessary physical evidence to interpret the observed non-conservative k_{eff} values and the inconsistency in the absorber effectiveness ranking between the different neutronic environments.

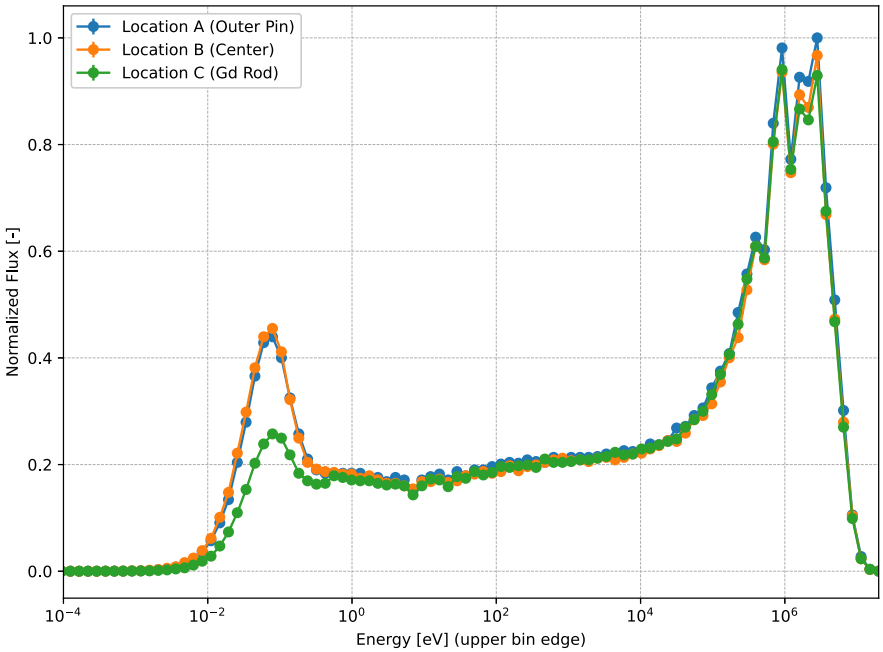

Figure 16: Normalized flux spectrum for the 3-Gd-rod case at Position 11 in the core model. Curves correspond to tally locations in Table 3 and are normalized according to the procedure described in Subsection 3.5.1.

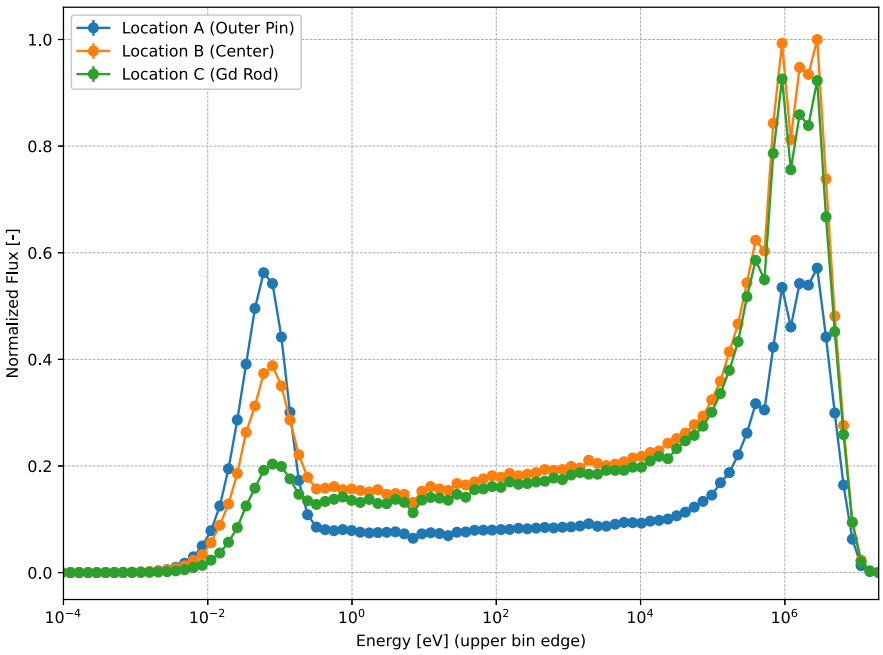

Figure 17: Normalized flux spectrum for the 3-Gd-rod case at Position 11 in the container model. Curves correspond to tally locations in Table 3 and are normalized according to the procedure described in Subsection 3.5.1.

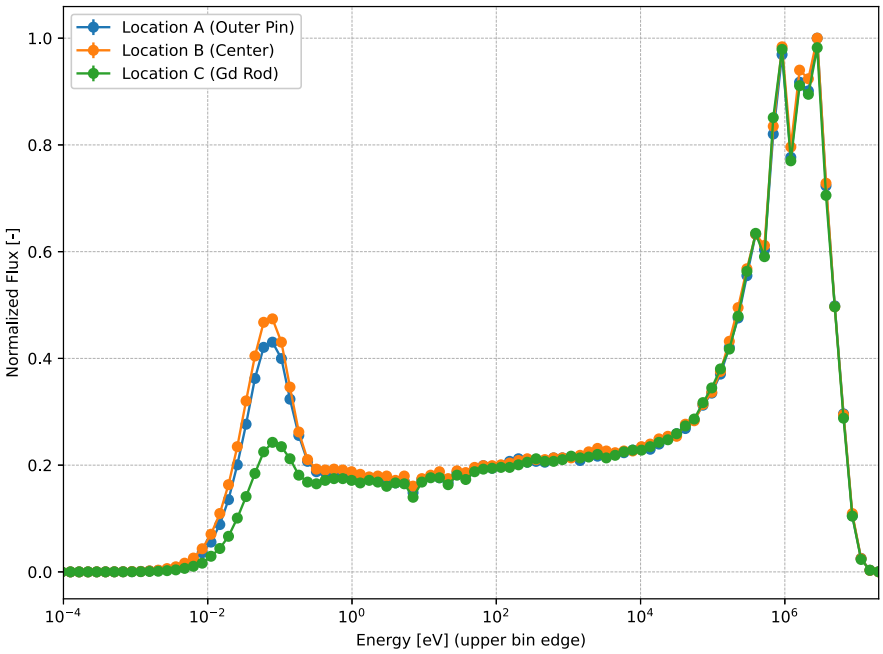

Figure 18: Normalized flux spectrum for the 3-Gd-rod case at Position 7 in the core model. Curves correspond to tally locations in Table 3 and are normalized according to the procedure described in Subsection 3.5.1.

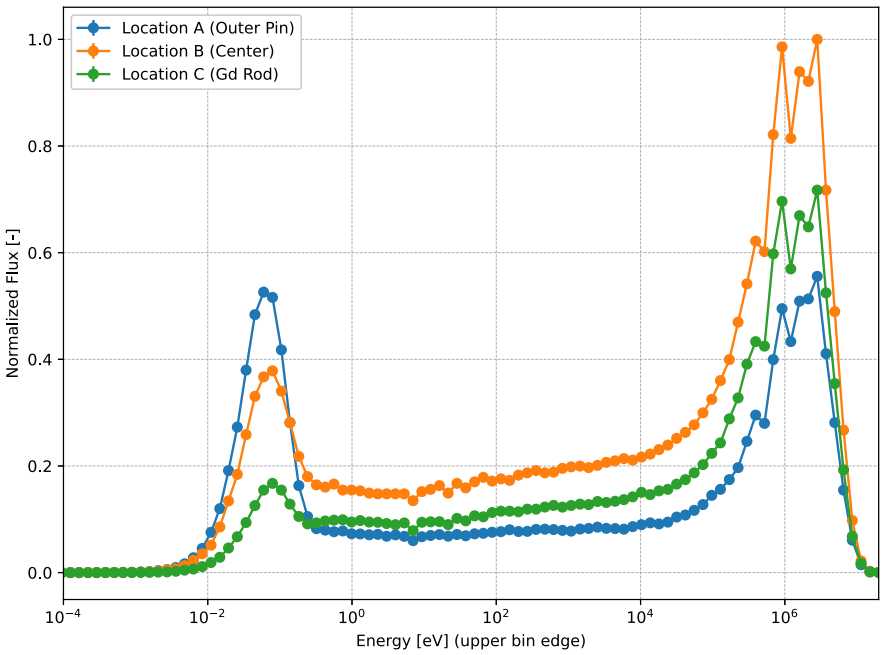

Figure 19: Normalized flux spectrum for the 3-Gd-rod case at Position 7 in the container model. Curves correspond to tally locations in Table 3 and are normalized according to the procedure described in Subsection 3.5.1.

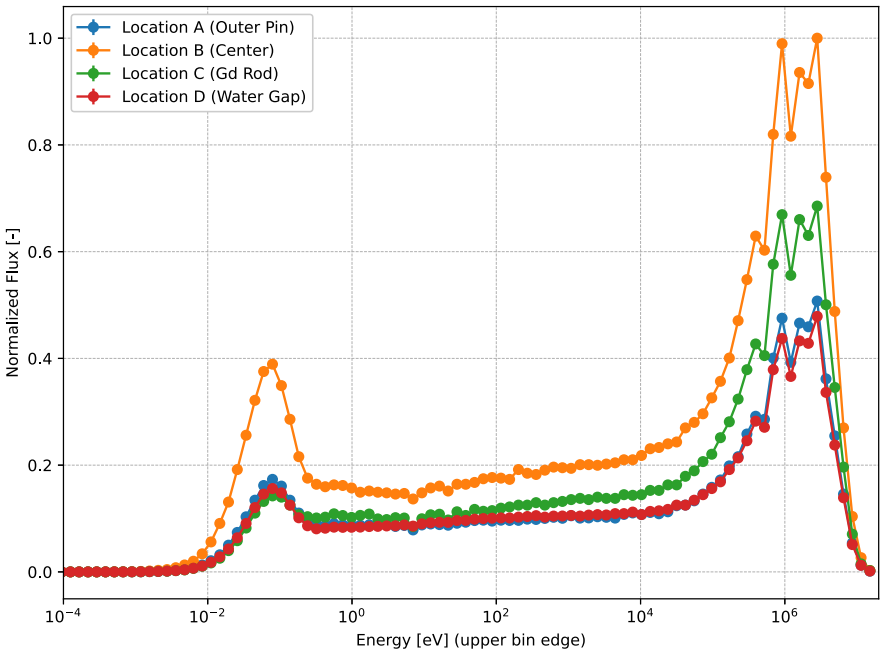

Figure 20: Neutron flux spectrum for the 3 Gd-rod case at Position 7 in the SFP model. Curves correspond to tally locations in Table 3 and are normalized according to the procedure described in Subsection 3.5.1.

5 Discussion

The numerical results in Chapter 4 demonstrate a systematic failure of the Reactivity Equivalence Method when a simplified core reference geometry is used to evaluate out-of-core storage configurations. The data show that the method is not only non-conservative, consistently underestimating the reactivity of the gadolinium-bearing fuel in the storage geometries, but is also unreliable, as it fails to identify the actual worst-case absorber configuration. This chapter provides the physical interpretation for these failures, which stem from two fundamental and interconnected neutronic phenomena: a non-linear competition between fuel enrichment and absorber worth driven by a global shift in the neutron spectrum, and a complete inversion of the spatial thermal flux profile within the fuel assembly.

5.1 Failure of Reactivity Equivalence Across Different Geometries

The primary failure of the Reactivity Equivalence Method is that it is non-conservative. Figure 8 and Figure 11 clearly demonstrate this, where the *equivalent* gadolinium-bearing fuel assemblies were found to be consistently more reactive than the reference fuel across all moderator densities in the 3D container geometry. This failure stems from a non-linear competition between two effects that are both highly sensitive to the neutron spectrum. The first effect is the positive reactivity from the higher $^{235}\mathrm{U}$ enrichment. The second is the negative reactivity from the gadolinium absorber.

As the spectral analysis shows (Figure 14 versus Figure 13), the container's larger lattice pitch creates a softer neutron spectrum than the core. As shown in Figure 1 and Figure 3, the fission cross-section of $^{235}\mathrm{U}$ and the absorption cross-sections for gadolinium isotopes are both higher in the thermal spectrum than in the fast spectrum. Therefore, when moving from core to container environment there is both a large positive reactivity gain for the higher-enrichment fuel and an increase of the negative reactivity worth of the gadolinium rods.

The Reactivity Equivalence Method fundamentally fails because these two effects do not scale proportionally. The equivalence was established in the harder-spectrum core model, where both the extra enrichment and the gadolinium had a relatively small neutronic impact. When moved to the softer-spectrum container, both effects are amplified, but the positive reactivity gain from the higher $^{235}\mathrm{U}$ enrichment is greater than the negative reactivity gain from the gadolinium's increased worth. The net result is that the *equivalent* FA becomes more reactive than the reference case, proving the method is non-conservative.

5.2 The Unreliability of Simplified Models: The Spatial Flux Inversion

Another critical finding of this analysis is that the simplified core model is fundamentally unreliable for safety analysis as it fails to identify the most reactive configuration of Gd-rods in the fuel assembly. Figure 12 provides clear evidence of this: the gadolinium rod pattern identified as the most reactive in the core model (Position 7) is, in fact, one of the least reactive in the 3D container geometry. Conversely, the most reactive pattern in the container (Position 11) was the least reactive in the core model. This critical inconsistency is a direct result of a spatial thermal flux inversion, which is clearly visible in the spectral analysis results.

The core model represents a tightly-packed lattice, where the neutron flux is slightly peaked towards the center, as shown in Figure 13. In contrast, Figure 14 shows that the container features a fuel assembly surrounded by a large volume of external water, which is the primary source of thermal neutrons, which subsequently diffuse inward into the assembly. This process creates a high thermal flux peak at the assembly's outer edge (Location A) and a depressed thermal flux at the center (Location B). This reversal of the thermal flux profile directly explains the inconsistency. Placing gadolinium rods at Position 7 (edge) in the container puts them in the region of highest thermal flux, making them maximally effective absorbers and resulting in a low assembly k_{eff}. Placing them at Position 11 (center) puts them in the region of lowest thermal flux, resulting in the highest assembly k_{eff}. This finding demonstrates that the simplified core model is not only non-conservative but is also misleading, as it selects the wrong absorber pattern as the bounding case for licensing.

5.3 The Complexity of the SFP Environment and the Failure of Equivalence

The reason why the Reactivity Equivalence Method fails significantly in the SFP lies in the presence of borated storage racks. Comparing the neutron spectrum at relevant locations for the reference fuel assembly in the core and in the SFP, available in Figure 13 and Figure 15, respectively, it can be observed that the neutron environment is significantly different. In the SFP configuration, both the fast and thermal neutron spectra are reduced at the periphery of the FA, in contrast to the core model. The fast flux depression is due to the larger SFP pitch, while the thermal depression is due to the highly absorptive boron racks capturing thermal neutrons in the water gap between the FA and the rack. The boron acts as a sink of thermal neutrons, which are essentially stolen from the FA. Consequently, the worth of a Gd rod placed in the peripheral Position 7 is significantly lower in the SFP environment than predicted in the simplified core model, where the peripheral flux depression is absent. This reduction in the internal BA worth by competitive absorption with the external boron rack means the positive reactivity from the higher uranium enrichment is no longer compensated, demonstrating that the core equivalence method is once again non-conservative.

5.4 Ethical and Sustainable Implications

This study addresses the ethical imperative of nuclear safety highlighted by historical accidents like Tokai-mura (discussed in Section 2.5). This work shows that simplified models may fail to capture dangerous reactivity peaks and contributes to preventing potential criticality events, safeguarding operational staff and the public. Furthermore, enabling the safe storage of higher-enrichment fuel supports the nuclear industry's transition to longer fuel cycles. This transition enhances both ecological and economic sustainability. In fact, it decreases the total volume of spent fuel generated per unit of energy produced (ecological benefit) and optimizes the use of existing storage infrastructure, avoiding the need for additional construction (economic benefit).

6 Conclusion

The objective of this thesis was to assess the validity of the Reactivity Equivalence Method for out-of-core storage of gadolinium-bearing VVER-1000 fuel. The study demonstrates that reliance on a simplified core reference geometry yields results that are both non-conservative and unreliable for storage configurations.

The analysis proves that the Reactivity Equivalence Method fails due to spectral inconsistencies between the reactor core and storage environments. The method consistently underestimates reactivity in the fresh fuel storage container. The shift to a softer neutron spectrum amplifies the positive reactivity gain from the higher $^{235}\mathrm{U}$ enrichment more than it amplifies the negative reactivity worth of the gadolinium. Furthermore, the simplified core model fails to identify the bounding absorber configuration. In the storage container, the spatial thermal flux profile peaks at the periphery rather than the center, contrarily to what happens in the core. Consequently, the gadolinium rod pattern identified as the most reactive in the core model (Position 7) is effectively the least reactive in the storage geometry, while the true worst-case configuration (Position 11) is missed. Moreover, in the SFP, competitive absorption between the internal gadolinium and external borated racks further reduces the absorber's effectiveness. This results in a significant reactivity increase for the equivalent fuel compared to the reference case.

These findings indicate that the Reactivity Equivalence Method based on in-core k_∞ is inadequate for licensing systems with spectrally sensitive absorbers. To ensure safety margins, criticality safety analyses for gadolinium-bearing fuel must use 3D models that accurately represent the moderation and spectral conditions of the specific storage environment. Additionally, the bounding absorber configuration must be determined within the actual storage geometry, as the rank of rod patterns is environment-dependent.

The validity of these conclusions is subject to specific conservative assumptions applied to ensure bounding results. Fissile materials were modeled with uniform enrichment and bounding manufacturing tolerances to maximize reactivity, while temperature feedback mechanisms were neglected by simulating at standard ambient conditions. Geometrically, the spent fuel pool analysis utilized an infinite lattice approximation; while this conservatively eliminates leakage, it precludes the assessment of macroscopic full-pool effects. Finally, the study focused exclusively on fresh fuel at its peak reactivity state, meaning the spectral hardening associated with fuel depletion was not explicitly modeled, though the fundamental failure mechanisms identified remain valid.

Future studies should address specific areas to refine the methodology and broaden the applicability of these findings. First, the spectral analysis should extend to irradiated fuel to determine if the spatial flux inversion and non-linear reactivity scaling persist at high burnup, where plutonium and fission products

buildup alter the neutron spectrum. Furthermore, future research could investigate the development of an empirical correction factor based on a spectral index, such as the ratio between thermal and fast flux. By correlating the observed reactivity bias with this measurable parameter, operators could mathematically compensate for the non-conservative spectral shift while retaining the computational efficiency of simplified equivalence calculations.

Bibliography

[1] J. C. Wagner, M. D. DeHart, and C. V. Parks. Technical Basis for Peak Reactivity Burnup Credit for BWR Spent Nuclear Fuel in Storage and Transportation Systems. Tech. rep. NUREG/CR-7194. ORNL/TM-2014/240. U.S. Nuclear Regulatory Commission, Apr. 2015.

[2] J.-C. Neuber. "Criticality Analysis of BWR Spent Fuel Storage Facilities Inside Nuclear Power Plants". In: Proceedings of the 6th International Conference on Nuclear Criticality Safety (ICNC'99). Siemens AG Power Generation Group. Versailles, France, 1999.

[3] Nuclear Energy Institute. Guidance for Performing Criticality Analyses of Fuel Storage at Light-Water Reactor Power Plants. Tech. rep. NEI 12-16, Revision 4. Washington, D.C.: Nuclear Energy Institute, Sept. 2019.

[4] C. J. Werner, J. C. Armstrong, et al. MCNP User's Manual - Code Version 6.2. Tech. rep. LA-UR-17-29981. Los Alamos National Laboratory (LANL), 2017. URL: https://rsicc.ornl.gov/codes/ccc/ccc8/ccc-850.html.

[5] S. G. Cho, K. I. Cha, and K. H. Cha. "Criticality safety analysis for eccentric loading of fuel assemblies in spent nuclear fuel cask". In: Nuclear Engineering and Technology 57 (2025), p. 103221.

[6] D. H. Park, S. U. Yoo, and C. J. Park. "Criticality analysis of the optimum moderation condition in the PWR fuel storage Facility". In: Annals of Nuclear Energy 213 (2025), p. 111175. ISSN: 0306-4549. DOI: https://doi.org/10.1016/j.anucene.2024.111175. URL: https://www.sciencedirect.com/science/article/pii/S0306454924008387.

[7] Electricity Information. Accessed: 2025-11-10. International Energy Agency. July 2025. URL: https://www.iea.org/data-and-statistics/data-product/electricity-information.

[8] Fact Sheet: Uranium Hexafluoride (UF6). Accessed: 2025-11-10. World Nuclear Transport Institute (WNTI), Sept. 2021. URL: https://www.wnti.co.uk/wp-content/uploads/2021/09/WNTI_Fact_Sheet_UF6_v3.pdf.

[9] Westinghouse Sverige. Produkter tjänster. https://westinghousenuclear.com/sweden/produkter-tjaenster/. Accessed: 2025-10-22.

[10] U.S. Nuclear Regulatory Commission. Stages of the Nuclear Fuel Cycle. Accessed: 2025-10-22. 2020. URL: https://www.nrc.gov/materials/fuel-cycle-fac/stages-fuel-cycle.

[11] International Atomic Energy Agency. Status and Trends in Spent Fuel and Radioactive Waste Management. Tech. rep. STI/PUB/1799. No. NW-T-1.14. Vienna: International Atomic Energy Agency, Jan. 2018. URL: https://www-pub.iaea.org/MTCD/Publications/PDF/P1799_web.pdf.

[12] D. A. Brown et al. "ENDF/B-VIII.0: The 8^{th} Major Release of the Nuclear Reaction Data Library with CIELO-project Cross Sections, New Standards and Thermal Scattering Data". In: Nuclear Data Sheets 148 (2018). Special Issue on Nuclear Reaction Data, pp. 1–142. ISSN: 0090-3752. DOI: https://doi.org/10.1016/j.nds.2018.02.001. URL: https://www.sciencedirect.com/science/article/pii/S0090375218300206.

[13] J. R. Lamarsh and A. J. Baratta. Introduction to Nuclear Engineering. 3rd edition. Upper Saddle River, NJ: Prentice Hall, 2001. ISBN: 978-0201824988.

[14] International Atomic Energy Agency. Criticality Safety in the Handling of Fissile Material. IAEA Safety Standards Series No. SSG-27 (Rev. 1). ISBN 978-92-0-131822-7. Vienna: International Atomic Energy Agency, 2022. URL: https://www-pub.iaea.org/MTCD/Publications/PDF/PUB1995_web.pdf.

[15] T. P. McLaughlin et al. A Review of Criticality Accidents, 2000 Revision. Tech. rep. LA-13638. Los Alamos National Laboratory (LANL), Los Alamos, NM (United States), 2000.

[16] World Nuclear Association. Tokaimura Criticality Accident 1999. https://world-nuclear.org/information-library/safety-and-security/safety-of-plants/tokaimura-criticality-accident.aspx. Accessed: 2025-10-21. Oct. 2020.

[17] J. A. Evans et al. Burnable Absorbers in Nuclear Reactors - A Review. Tech. rep. INL/JOU-21-61443-Rev-0. Idaho National Laboratory (INL), May 2022. DOI: 10.2172/1868953. URL: https://www.osti.gov/servlets/purl/1868953.

[18] Westinghouse Electric Company. VVER-1000 Fuel Products. Product Specification Sheet. Available at: https://www.westinghousenuclear.com/media/vi0p2out/vver-1000-fuel-products.pdf. 2018.

[19] Westinghouse Electric Company report WCAP-14111, "Criticality Analysis of the Temelín Fresh Fuel Storage Containers and Spent Fuel Storage Racks", Rev 0. Dec. 1994.

[20] F. B. Brown, M. E. Rising, and J. L. Alwin. Verification of MCNP6.2 for Nuclear Criticality Safety Applications. Tech. rep. Los Alamos National Lab. (LANL), Los Alamos, NM (United States), May 2017. DOI: 10.2172/1356287. URL: https://www.osti.gov/biblio/1356287.

[21] Westinghouse Electric Sweden report WSE0028160, "MCNP6.2 Validation for Criticality Calculations: Homogeneous Systems". Feb. 2023.

[22] Westinghouse Electric Sweden report WSE0033178, "MCNP6.2 Validation for Criticality Calculations: Heterogeneous Systems". Aug. 2023.

[23] X-5 Monte Carlo Team. MCNP-A General Monte Carlo N-Particle Transport Code, Version 5, Volume I: Overview and Theory. Tech. rep. LA-UR-03-1987. Los Alamos National Laboratory, 2003.

[24] Westinghouse Electric Sweden report WSE0056549, "Criticality Analysis of the Temelín Fresh Fuel Storage Containers and Spent Fuel Storage Racks for RWFA-T Fuel", Rev 0, Draft B. Nov. 2024.